Insensitive Munitions Formulations: Their Dissolution and Fate in Soils

Susan Taylor, Katerina Dontsova and Marianne Walsh

Abstract New explosive compounds that are less sensitive to shock and high temperatures are being tested as replacements for TNT (2,4,6-trinitrotoluene) and RDX (hexahydro-1,3,5-trinitro-1,3,5-triazine). Two of these explosives, DNAN (2,4-dinitroanisole) and NTO (3-nitro-1,2,4-triazol-5-one), have good detonation characteristics and are the main ingredients in a suite of insensitive munitions (IM) explosives. Both compounds, however, are more soluble than either TNT or RDX. Data on their fate could help determine if DNAN and NTO have the potential to reach groundwater and be transported off base, an outcome that could create future contamination problems on military training ranges and trigger regulatory action. In this chapter, we describe how quickly IM constituents (DNAN, NTO, nitroguanidine, RDX and ammonium perchlorate) dissolve from three IM formulations (IMX-101, IMX-104 and PAX-21) and how solutions of IM compounds interact with different types of soils. This information, coupled with the mass of IM formulations scattered on a range, will allow estimates of the dissolved IM mass loads, their subsequent transport and fate, and their likelihood of reaching groundwater.

Keywords High explosives · Dissolution · Soil interactions

1 Introduction

New explosive compounds that are less sensitive to shock and high temperatures are being tested as replacements for TNT (2,4,6-trinitrotoluene) and RDX (hexahydro-1,3,5-trinitro-1,3,5-triazine). Two of these explosives, DNAN (2,4-dinitroanisole) and NTO (3-nitro-1,2,4-triazol-5-one), have good detonation

S. Taylor (✉) · M. Walsh
Cold Regions Research and Engineering Laboratory, Hanover, NH 03766, USA
e-mail: Susan.Taylor@erdc.dren.mil

K. Dontsova
Biosphere 2, University of Arizona, Tucson, AZ 85721-0158, USA

characteristics and are the main ingredients in a suite of insensitive munitions (IM) formulations that are being fielded (Table 1). Both compounds, however, are more soluble than either TNT or RDX (Table 2) and research has shown that both have some human and environmental toxicity. Toxicology data for DNAN show that it is more toxic to mammals than TNT [1–3], can inhibit seed germination and plant growth [4] and is toxic to bacteria and earthworms [5]. While NTO has low mammalian toxicity [6], both DNAN and NTO can form toxic transformation products [3, 7, 8].

Explosives are released onto training range soils when unexploded ordnance (UXO) casings fail and after incomplete (partial) detonations during training with explosive-filled munitions and from blow-in-place operations. Partial detonations are estimated to deposit most of the explosive mass available for dissolution on ranges today [9]. The solid particles of IM explosives, scattered by incomplete detonations, are dissolved by precipitation and can then travel to groundwater. What compounds reach grosundwater is determined by their rates of dissolution, photo-transformation (both in solid form and in aqueous solution), and complex interactions of the aqueous explosive solutions with soil constituents during transport through the vadose zone.

Solubility, along with particle size and climatic conditions (rainfall and temperature), controls the dissolution rate of solid explosives [10–12]. The solubility of DNAN and nitroguanidine (NQ) increases by a factor of two between 20 and 40 °C and almost doubles for NTO (Fig. 1). The dissolution of DNAN and NTO, when part of a formulation, will depend not only on their individual solubility but also on the fraction of each component exposed to water. This process has been documented and modeled for high explosives [13, 14, 10, 11, 12]) but is different for DNAN-based IM formulations. The latter have constituents with order of magnitude differences in solubility, resulting in, not smaller diameter particles as occurs for HE, but hole-riddled particles with the same initial diameter [15, 16]. DNAN composes the matrix of IM formulations and, as it is one of the least soluble components, it persist as porous particles subject to photo-transformation. It is likely that their surfaces will photo-transform in the environment and, if the products are soluble, that these compounds could travel with the precipitation into the soil and possibly to groundwater.

Table 1 Compositions of IM formulations (IMX-101, IMX-104 and PAX-21) that contain DNAN and NTO and that we studied

IM	Components	Used in
IMX-101	DNAN, NQ, NTO	Qualified as the main fill in the 155 mm projectile
IMX-104	NTO, DNAN, RDX	Used by the U.S. Army for 60, and 81 mm mortars
PAX-21	DNAN, AP, RDX	No longer being fired during training or testing on US ranges

RDX contains about 10% HMX (octahydro-1,3,5,7-tetranitro-1,3,5,7-tetrazocine) as a manufacturing impurity. Data are from Fung et al. [17], Wilson [18], Pelletier et al. [19], and Coppola [20]

Table 2 Properties of DNAN, NTO and other compounds found in IM formulations

Energetic	Aqueous solubility[a]	Density	Formula	Reference
DNAN	276	1.34	$C_7H_6N_2O_5$	[21]
NTO	16,642	1.93	$C_2H_2N_4O_3$	[22]
TNT	128	1.65	$C_7H_5N_3O_6$	[23]
RDX	56	1.82	$C_3H_6N_6O_6$	[24]
HMX	4.5	1.81	$C_4H_8N_8O_8$	[24]
NQ	2600 ± 100	1.55	$CH_4N_4O_2$	[25]
AP	217,000	1.95	NH_4ClO_4	[26]

[a]mg L^{-1} at 25 °C

Fig. 1 Aqueous solubility of **a** DNAN, **b** NQ and **c** NTO plotted as a function of temperature
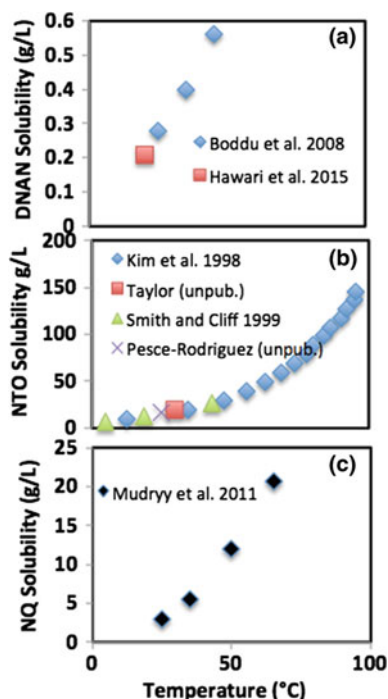
2 Field Deposition

Military training scatters explosive and propellantcompounds onto the soil surface. As was discussed for HE[13], the mass of the scattered materials depends on the type of round fired and the manner in which it detonated: high-order, low-order (partial), or blow-in-place detonations. IM formulations are mainly being used to fill mortar rounds and artillery projectiles (Table 1). Table 3 summarizes detonation test results for similar caliber rounds filled with either IM or HE. For the high order tests, rounds were either fired or command detonated using a fuze simulator [27].

Table 3 Comparison of IM and HE residues deposited after high-order and blow-in-place detonations, data from Walsh et al. [28, 29, 30, 27, 31]. The high order detonation residues were collected from either fired rounds or command detonations that initiated the normal detonation chain of the round. The blow in place detonations used one or more C4 blocks placed on the outside of the round-the current EOD practice

		Residue deposited		High Order				blow-in-place						
Caliber	Dodic	# sampled	Exp. Fill	Compounds	Mass (g)	Residues (mg)	Exp. Consumed Efficiency (%)	Dodic	# sampled	Exp. Fill	Compounds	Mass (g)	Residues (mg)	Exp. Consumed Efficiency
Mortar 60-mm	M888	7	Comp B	TNT	153	nd	100.000	M888 Block C4	7	Comp B	TNT	750	200	99.973
				RDX+HMX	230	0.073	100.000				RDX+HMX			
	M888	5	Comp B	TNT	153	nd	100.000							
				RDX+HMX	230	0.074								
	M768	7	PAX 21	DNAN	120	7.1	99.994	M768 Block C4	7	PAX 21	DNAN	120	7.1	99.994
				RDX+HMX	130	9.2	99.993				RDX+HMX	130	9.2	99.993
				AP	91	14,000	84.615				AP	91	14,000	84.615
				Total	341	14016.3	95.890				Total	341	14016.3	95.890
		7	IMX-104	DNAN	110	5.3	99.995	No dodic Block C4	7	IMX-104	DNAN	110	20120	81.709
				NTO	180	2200	98.778				NTO	180	89000	50.556
				RDX+HMX	75	4.5	99.994				RDX+HMX	600	8300	98.617
				Total	365	2209.8	99.395				Total	890	117420	86.807
81-mm	M374	14	Comp B	TNT	400	nd	99.999	M374 block C4	7	Comp B	TNT	1100	150	99.986
				RDX+HMX	600	8.5	99.998				RDX+HMX			
	M374	3	Comp B	TNT	400	nd								
				RDX+HMX	600	10								
	M821A2 12g C4	7	IMX-104	DNAN	260	27	99.990	M821A2 block C4	7	IMX-104	DNAN	260	45000	82.692
				NTO	430	1900	99.558				NTO	430	230000	46.512
				RDX+HMX	150	16	99.989				RDX+HMX	680	20000	97.059
				Total	840	1943	99.769				Total	1370	295000	78.467
	M821A2 18g C4	5	IMX-104	DNAN	260	7.8	99.997	M821A2 block C4	7	IMX-104	DNAN	260	5000	98.077
				NTO	430	540	99.874				NTO	430	45000	89.535
				RDX+HMX	160	7.6	99.995				RDX+HMX	860	2100	99.756
				Total	850	555.4	99.935				Total	1550	52100	96.639
	M821A2 18g C4	1	IMX-104	DNAN	260	13	99.995							
				NTO	430	1150	99.733							
				RDX+HMX	160	3.8	99.998							
				Total	850	1166.8	99.863							
	M821A2 18g C4	2	IMX-104	DNAN	260	17	99.993							
				NTO	430	720	99.833							
				RDX+HMX	160	4.1	99.997							
				Total	850	741.1	99.913							
120-mm	M933	7	Comp B	TNT	1800	19	99.999	M933 Block C4	7	Comp B	TNT	2300	25	99.999
				RDX+HMX							RDX+HMX			

Table 3 (continued)

Caliber	Dodic	# sampled	Exp. Fill	Compounds	Mass (g)	Residues (mg)	Exp. Consumed	# sampled	Exp. Fill	Compounds	Compounds	Mass (g)	Residues	Exp. Consumed
		Residue deposited						High Order			blow-in-place			
Howitzer 105-mm	M1	9	Comp B	TNT	1300	0.095	100.000	7	Comp B	M1	TNT	1800	50	99.997
				RDX+HMX						Block C4	RDX+HMX			
155-mm	M107	7	Comp B	TNT	4200	0.3	100.000	7	Comp B	M107	TNT	4700	15	100.000
				RDX+HMX						Block C4	RDX+HMX			
155-mm practice	M107	7	TNT	TNT	6600	nd	100.000	7	TNT	M107	TNT	6600	5.9	100.000
										Block C4	RDX	520	5.9	99.999
	M1122 40-g C4	1	IMX-101	DNAN	480	5900	98.771	3	IMX-104	M1122	DNAN	480	5300	98.896
				NTO	230	40000	**82.609**			Block C4	NTO	230	15000	93.478
				NQ	430	170000	**60.465**				NQ	430	100000	76.744
				RDX+HMX	40	18	99.955				RDX+HMX	710	21	99.997
				Total	700	210018	69.997				Total	1370	115021	91.604
	M1122 50-g C4	7	IMX-101	DNAN	480	2400	99.500	7						
				NTO	230	15000	93.478							
				NQ	430	130000	**69.767**							
				RDX+HMX	50	12	99.976							
				Total	710	145012	79.576							
	M1122 60-g C4	1	IMX-101	DNAN	480	660	99.863	3	IMX-104	M1122	DNAN	480	21000	95.625
				NTO	230	14000	93.913			2 blocks C4	NTO	230	24000	89.565
				NQ	430	120000	**72.093**				NQ	430	100000	76.744
				RDX+HMX	50	10	99.980				RDX+HMX	1200	46	99.996
				Total	710	134010	81.125				Total	1860	124046	93.331
120-mm	100-g C4	5	PAX-21	DNAN	1700	nd		5	PAX-21	5 blocks C4	DNAN	1700	53000	96.882
				NTO	1100	23	99.998				NTO	1100	410000	62.727
				RDX+HMX	740	nd					RDX+HMX	3300	3800	99.885
				Total	3540	23	99.999				Total	6100	466800	92.348

TNT (2,4,6-trinitrotoluene), RDX (hexahydro-1,3,5-trinitro-1,3,5-triazine), HMX (octahydro-1,3,5,7-tetranitro-1,3,5,7-tetrazocine), NQ (nitroguanidine), NTO (3-nitro-1,2,4-triazol-5-one), DNAN (2,4-dinitroanisole). Explosive fill (Exp. Fill) refers to the type of explosive formulation in the round

C4 in the simulator is detonated using a blasting cap and this blast initiates the detonation train of the round. For the blow-in-place tests, C4 blocks were placed on the outside of the round following the procedure used by explosive ordnance disposal personnel. The data show that more IM residue is deposited than HE residue for similar detonation conditions. For HE high order detonations 99.99% of the mass in the rounds is consumed but this percentage is slightly lower for most IM detonations and much lower for their individual constituents-values in bold highlight the lower percentage of ammonium perchlorate consumed (84%) in PAX-21, and the lower percentage of NTO (83–94%) and NQ (60–72%) consumed for IMX-101-filled rounds. The NTO consumed in IMX-104 rounds was consistently higher (>99.5%) for high order detonations but much lower and more variable for the blow-in-place detonations (47–90%). The IM blow-in-place detonations left more residues, particularly their crystal constituents AP, NQ and NTO, than did the HE blow-in-place (Table 3). It should be noted that the US Army has discontinued training using PAX21-filled rounds because of the amount of AP they deposit.

The field deposition of IM formulations differs from that of HE in two significant ways. First of all, IM rounds are designed to be more difficult to detonate and they leave more residues. Secondly, a fraction of the NTO, NQ and AP crystals in the DNAN matrices is deposited on the soil, even during high order detonations (Table 3). Micro computed tomographic (μCT) images show that the constituent crystals are de-bonded from the DNAN matrix during detonation, allowing some fraction of the crystals to be scattered (Fig. 2) [15].
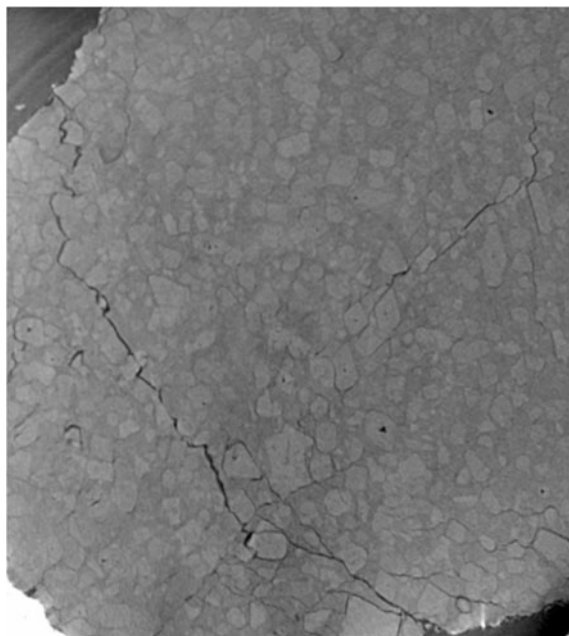
Fig. 2 A micro computed tomography (μCT) image of an IMX-101 particle from a partial detonation. Note that the fractures tend to travel through the DNAN matrix and around the periphery of both the NTO and NQ crystals
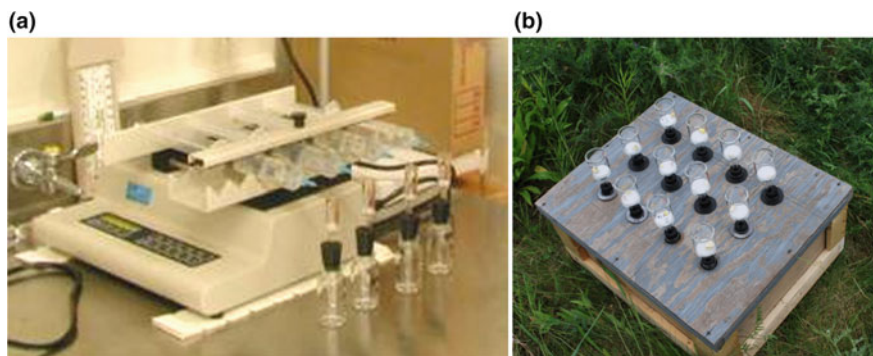
Fig. 3 Photos of **a** the laboratory drip tests and **b** the outdoor setup where glass liter jars in the box collect the effluent from precipitation interacting with explosive pieces in the glass funnels

3 Dissolution of IM Detonation Residues

3.1 Indoor Drip Tests

Taylor et al. [32] used well-controlled laboratory drip experiments to obtain dissolution data on field collected particles of IMX-101, IMX-104, and PAX-21 from detonation experiments [29, 31]. The laboratory tests used massed individual mm-size pieces of the explosive placed on a glass frit and dripped on by water at a 0.5 mL/h (Fig. 3a), after which the effluent was analyzed using HPLC. The laboratory tests on IMX-101 particles showed that NTO was the first compound to dissolve followed by NQ, and DNAN, (Fig. 4 top) consistent with the solubility of each component (Table 2; Fig. 1). NTO was lost quickly as indicated by a steep rise in the mass loss curve followed by a flat plateau. NQ had a less steep initial rise but also reached a plateau. DNAN was the last component to dissolve. The mass loss curves for the four IMX-104 particles (Fig. 4 bottom) show that NTO was again dissolved rapidly. The percent mass loss curves for the DNAN matrix were fairly linear with a larger percentage of DNAN dissolving early in the test and a larger fraction of RDX dissolving later in the test. These results agree with those obtained on a single, 150 mg piece of IMX-101 that was similarly dissolved [32, 33].

The mass balances for the indoor IMX-101 and IMX-104 tests show that the formulations are not being significantly photo- or bio-transformed in the laboratory because most of the mass ($100 \pm 5\%$) was recovered [15]. If these IM formulations were transforming into new, unknown compounds, the mass balance would be poor.
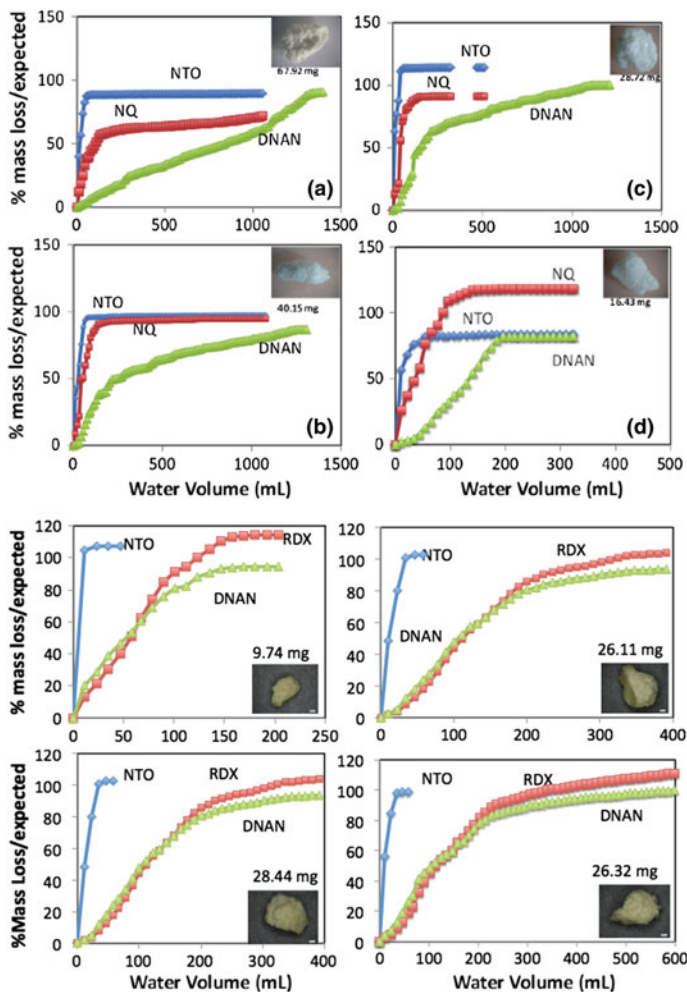
Fig. 4 Top four panels show the percent of mass dissolved for compounds in IMX-101 versus water volume (mL) and the bottom four panels show the same information for IMX-104. The y-axis plots the percent mass loss measured by HPLC relative to the expected mass (mass of initial particle multiplied by the percent contribution of each constituent in the formulation). Drip rate was 0.5 mL/h [25]

3.2 Outdoor Dissolution Tests

For the outdoor dissolution tests millimeter to centimeter-size chunks of detonated IM explosives were placed outside to weather under natural conditions (Fig. 3b); five particles of IMX-101 (#1 to #5), five particle of IMX-104 and two particles of PAX-21. The experiment ran for 864 days during which time the samples were wetted by 147 cm of precipitation. These tests simulated the dissolution of isolated

IM pieces on range soils and can be scaled based on rainfall rates at other locations. No soil was involved in any of the tests, yielding dissolution as a function of the particle mass and the water volume, average 3.7 ± 0.27 L, interacting with each particle [15, 16, 32].

The formulations were initially white (IMX-101), cream colored (IMX-104) and yellow (PAX-21) but their surfaces turned yellow after two weeks and orange to brick red after a year of exposure to sunlight (Fig. 5). During the 864 day long dissolution test all of the IM chunks split and all shed mm-sized particles, a much faster splitting rate than observed during similar tests on TNT, Comp B and Tritonal (TNT + aluminum) (Fig. 6) [34]. The friability of the IM formulations could be due to: (1) the large, ~ 300 μm, crystals they contain; (2) the voids left when the crystals dissolve or; (3) to fractures produced during detonation (Fig. 7) [32]. All of these features could weaken the IM formulations. The μCT images of an IMX-101 and an IMX-104 chunk taken before, part way through, and at the end of the outdoor tests (Fig. 7a, b) show that IMX-101 has lost crystals in its interior and periphery but less so than IMX-104 where all the NTO crystals dissolved.

Figure 8 shows the percent cumulative mass dissolved for each constituent in the IM formulation plotted against the cumulative volume of water collected. The mass loss data for the five IMX-101 chunks show that NTO dissolves first, followed by NQ and finally DNAN (Fig. 8a). The dissolution rates of NTO and NQ are higher at
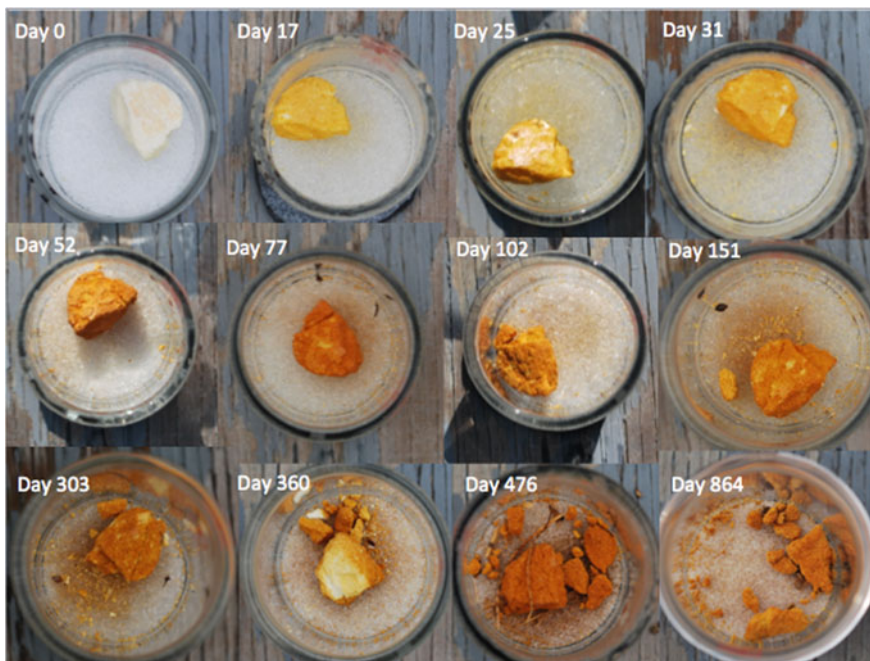
Fig. 5 IMX-101#1, set outside to weather and dissolve, shows changes to the appearance of the particle over the 864 days of the experiment
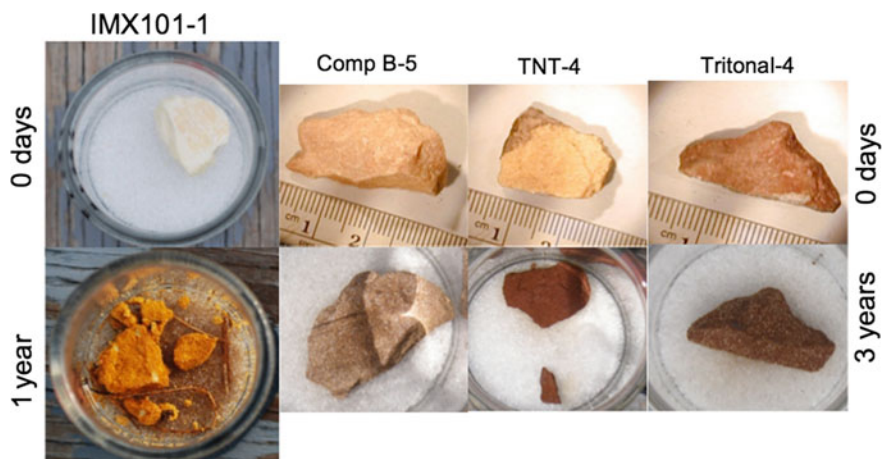
Fig. 6 IM formulations are very friable compared to traditional explosives
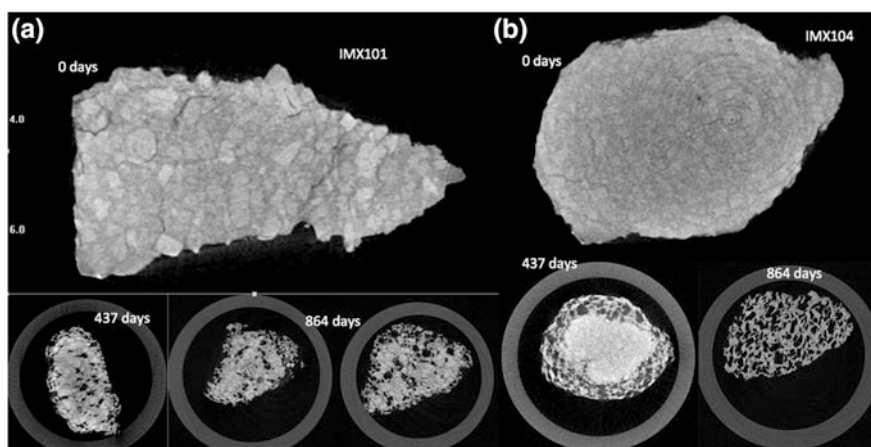
Fig. 7 Micro computed tomography (μCT) cross-sections of IMX-101 (**a**), and IMX-104 (**b**) taken at 0 and 437 and 864 days. These particles split during the test so the images taken at day 437 and 864 are the largest fragments of the original chunk

the start of the test and decrease with time. The shape of the NTO mass loss with water volume curve is more clearly seen for IMX-104, which contains no NQ (Fig. 8b). Figure 8c shows that the AP in PAX 21 dissolved in the first water sample indicating that water was able to access the interior of the PAX-21 particle.

As was found for laboratory experiments [33, 32], the constituents of the formulations dissolve in the order of their solubility. None of these chunks had completely dissolved after 864 days.
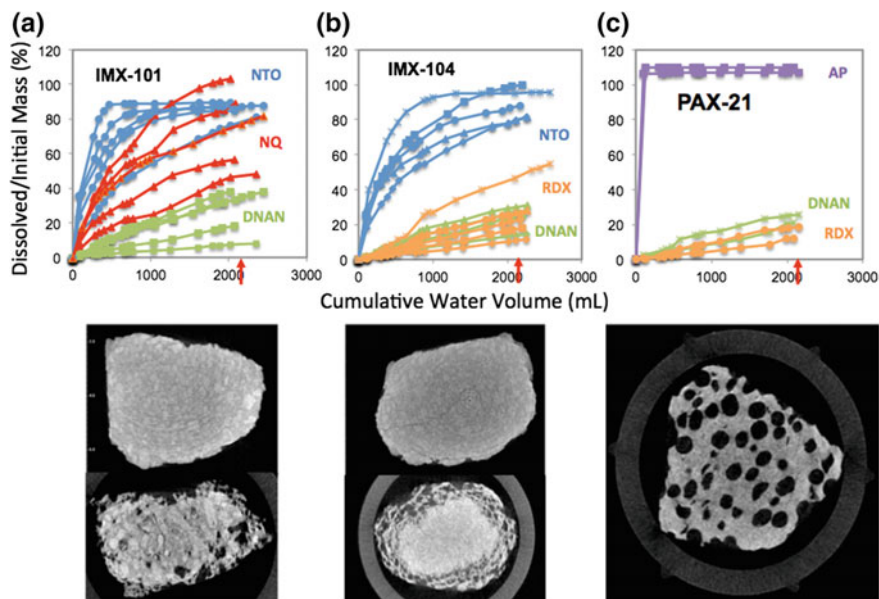
Fig. 8 Dissolved mass versus precipitationvolume for 5 IMX-101 (**a**), 5 IMX-104(**b**) and 2 PAX-21 (**c**) chunks placed outside, NTO (*blue*), NQ (*orange*), DNAN (*green*), RDX (*red*), AP (*purple*) [16]. Micro computed tomography images were taken at the beginning and near the end of the tests (*red arrows*). No initial µCT image for the PAX-21 is shown because the AP crystals appear very bright and produce artifacts and a poor quality image

Unlike TNT and Comp B, IM formulations dissolve throughout their volumes due to their soluble crystals constituents. One cannot, therefore, use dissolution models that assume dissolution from the surface [10] to calculate particle lifetimes. In these formulations, however, DNAN (and RDX) dissolve at a semi-constant rate; the mass loss is fairly linear when plotted against water volume (Fig. 9). The best linear fits to the DNAN data have slopes ranging from 0.0114 to 0.0572 and goodness of fit measures (R^2) between 0.94 and 0.99. As DNAN constitutes the matrix, its quasi-linear dissolution can be used to estimate chunk lifetimes. IMX-101 particles of 0.3–3.5 g (0.6–1.4 cm) are estimated to need 6–27 L (240–1080 cm) of precipitation to dissolve so their persistence can be estimated from local rainfall records. Values are similar for IMX-104, where 0.2–2 g (0.5–1.1 cm) particles require 4–15 L (160–600 cm) of precipitation to dissolve and for PAX-21 where 0.2–1.3 g (0.5–1 cm) particles would need 7–11 L (280–1080 cm) of precipitation to dissolve.

Quasi-linear dissolution does not occur for the NTO or NQ, for mm-sizes particles of these formulations [15, 16], or for Comp B and TNT [12]. In all these cases the explosive pieces lose more mass initially when soluble constituents are at or near the surface of the chunk, and then mass loss decreases as constituents are depleted or as water has a harder time contacting the constituents. For DNAN, its
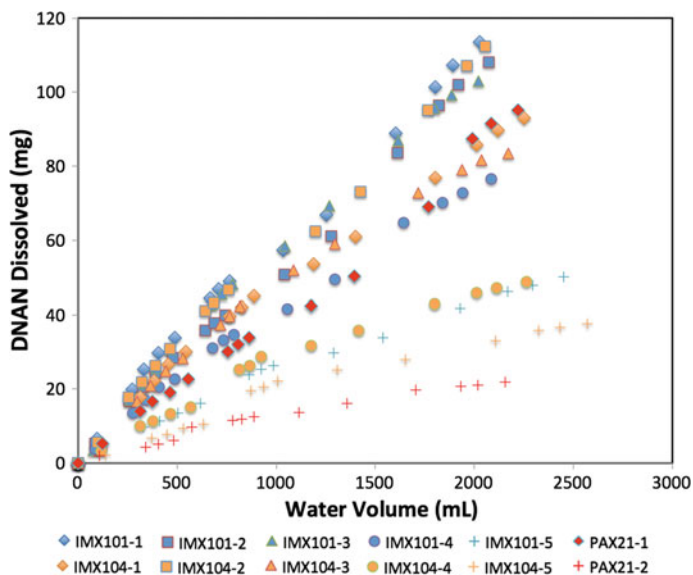
Fig. 9 Dissolved DNAN plotted against water volume for outdoor samples of IMX-101, IMX-104 and PAX-21 [11]

low solubility coupled with increases in its surface area explains the linear mass loss. When the IM chunks split, the numerous fragments that result increase the DNAN surface area and dissolution. This idea is supported by the fact that more fragments result in a better linear fit to the mass loss versus water volume data [15, 16]. Although fragmentation also affects the dissolution of NTO, NQ and AP none of these show quasi-linear dissolution because the time scales over which these compounds dissolve are shorter than the fragmentation rate.

3.3 Mass Balance for Outdoor Tests

Table 4 lists the initial and final masses for the IM particles, the difference between these masses, and how much explosive mass was found in the effluent samples. The same data for the high explosives (HE) outdoor tests is also shown. For IM, the difference between the initial and final masses averaged 0.8 ± 0.6 g and about 80% of this value was recovered in the effluent samples suggesting a 20% loss via photo-transformation. The conventional explosives (TNT, Comp B, Tritonal and C4) lost less mass, the difference between the initial and ending mass averaged 0.2 ± 0.08 g (constituents less soluble and particle less friable) but of this only about 20% was recovered in the effluent samples. This suggests that $\sim$ 80% was photo-transformed into compounds not analyzed for in the effluent samples [34].

Table 4 Results of mass balance calculation for IM and high explosive formulations

Insensitive munition formulations							High explosive formulations						
Sample	M_i (g)	M_f (g)	Diff (g)	M_{diss} (g)	M_{miss} (g)	M_{diss} (Diff)	Sample	M_i (g)	M_f (g)	Diff (g)	M_{diss} (g)	M_{miss} (g)	M_{diss} (Diff)
IMX-101-1	3.55	1.43	2.12	1.65	0.48	0.78	TNT-1	1.97	1.75	0.22	0.071	0.15	0.32
IMX-101-2	1.39	0.28	1.11	0.75	0.36	0.68	TNT-2	0.4	0.31	0.10	0.033	0.06	0.34
IMX-101-3	0.63	0.02	0.61	0.49	0.12	0.80	TNT-3	0.52	0.28	0.24	0.074	0.16	0.32
IMX-101-4	0.53	0.04	0.49	0.38	0.11	0.77	Comp B-1	0.78	0.65	0.13	0.065	0.06	0.50
IMX-101-5	0.31	0.05	0.26	0.23	0.03	0.89	Comp B-2	0.43	0.31	0.11	0.056	0.06	0.50
IMX-104-1	2.00	0.70	1.30	1.15	0.15	0.88	Comp B-3	5.07	4.85	0.22	0.066	0.15	0.30
IMX-104-2	1.42	0.13	1.29	0.99	0.30	0.77	Trit-1	2.97	2.77	0.20	0.047	0.16	0.23
IMX-104-3	0.99	0.23	0.76	0.65	0.11	0.86	Trit-2	5.32	4.99	0.33	0.054	0.28	0.16
IMX-104-4	0.49	0.13	0.36	0.33	0.03	0.91	Trit-3	2.47	2.22	0.24	0.054	0.19	0.22
IMX-104-5	0.22	0.01	0.21	0.18	0.03	0.85	C4-1	4.93	4.62	0.31	0.037	0.27	0.12
PAX-21-1	1.28	0.41	0.87	0.67	0.20	0.77	C4-2	3.97	3.64	0.33	0.059	0.27	0.18
PAX-21-2	0.25	0.08	0.17	0.14	0.03	0.80	C4-3	2.30	2.10	0.20	0.030	0.17	0.15

Initial (M_i) and final (M_f) masses of the particles

Diff = M_i − M_f

M_{diss} = Mass determined from effluent samples via HPLC

M_{miss} = Mass missing = M_i-(M_f + M_{diss})

HPLC mass/mass not recovered = (M_{diss})/(M_i − (M_f + M_{diss})

3.4 Photo-Transformation of IM

Photo-transformation is an important process because sunlight might chemically alter the surface of a compound to produce other compounds with different solubilities or toxicities. Hydrolysis studies found that without sunlight, DNAN and NTO are stable over a range of neutral, acidic, and basic conditions that can be encountered in natural environment and hydrolyze only at pH $\geq$ 12 (R. Pesce-Rodriguez, unpublished data [35, 36].

DNAN transformation pathways and products have been reported for several matrices including cell cultures, soil microcosms, sludge bioassays, treated wastewater, toxicity test organisms, irradiated aqueous solutions, and oxic aqueous solutions [8]. Few studies have been reported on the photo-transformation of the surface of solid pieces of DNAN or IM compositions [15]. Unknown peaks in the HPLC chromatograms of outdoor samples suggest that the particle surfaces are photo-degrading and forming new compounds; note the many additional peaks in Fig. 10. Some of the unknown peaks were not consistently present in effluent from these outdoor samples suggesting they were transient and actively transforming into other compounds.

A few studies report on photo-transformation products in DNAN aqueous solutions. Both Hawari et al. [37] and Rao et al. [38] found 2-methoxy-5-nitrophenol and 2,4-dinitrophenol as intermediates, and nitrate and, or nitrite or both (the analytical

Fig. 10 NovaPak C8 column chromatograms (absorbance at 230 nm) for; **a** an IMX-104 indoor drip sample (no sunlight exposure) and **b** an IMX-104 outdoor test. DNAN, RDX and HMX peaks are present but there are many unknown peaks and a large pre-solvent peak (*arrow*) in the outdoor sample
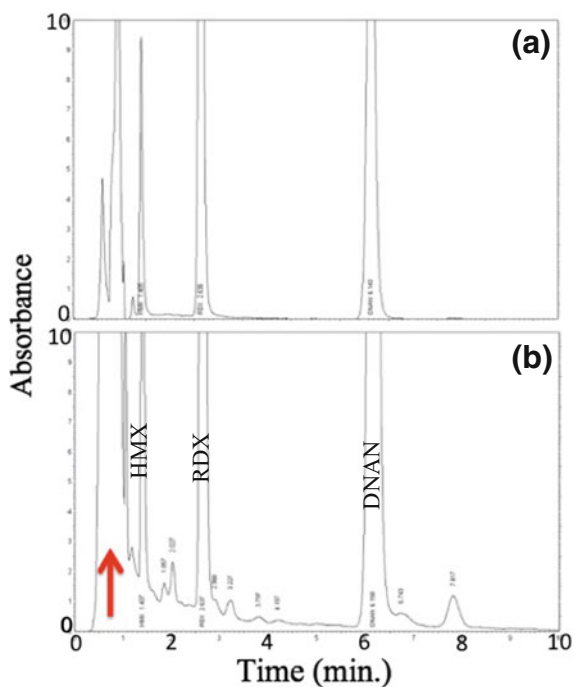
techniques could not separate the compounds). Hawari et al. [37] also reported formamide derivatives as intermediates of the transformation of amino-nitroanisole and amino-nitrophenol. The final products of a DNAN aqueous solution photolyzed over 21 days were, nitrate anion (0.7 mol), ammonium (1 mol), and formaldehyde/formic acid (0.9 mol, compounds also not separated), per mole of DNAN degraded [37]. Rao et al. [38] observed photo-transformation and a half-life ranging between 0.11 and 1.51 days. Observed products of photo-transformation for NTO, according to Le Campion et al. [39], include nitrites, nitrates, and carbon dioxide.

Taylor et al. [40] investigated thephoto-transformation of DNAN both as a pure solid and as a componentof solid IM formulations, IMX-101, IMX-104 and PAX-21. The latterwere samples placed outside to dissolve and transform as part of atwo and a half year dissolution study [16]. Taylor et al. [40] saw transient peaks in the chromatograms indicating intermediate, unstable products but consistently found methoxy nitrophenols and methoxy nitroanilines. One unknown product, possibly nitrosobenzene, was also found in most of the samples. The concentrations of transformation products found were small, <1% of the dissolved DNAN concentration, suggesting that DNAN, not its transformation products, will be the main compound entering the soil.

The effect of temperature, pH, and dissolved organic matter on photo-transformation of DNAN and NTO in solution was examined by Dr. R. Pesce-Rodriguez [41]. The NTO transformation rates depended on the solution pH (Fig. 11a), with the lowest rates observed at neutral pH. The NTO photo-transformation rate doubled in the presence of humic acid (Fig. 11b), but was not affected by temperature (Fig. 12). Photo-transformation of DNAN in solution, on the other hand, was not sensitive to pH or natural organic matter but increased with increasing temperature (Fig. 12) a finding also reported by Rao et al. [38]. This suggests that DNAN may be less persistent in hot climates. The calculated activation energy for DNAN photo-transformation was 27.8 kJ mol^{-1} [41].
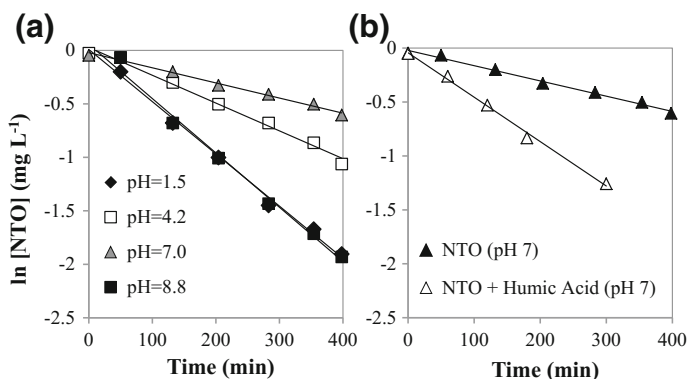
Fig. 11 Photo-transformation of NTO as affected by **a** solution pH and **b** the presence of natural organic matter [41]

Fig. 12 Measured (*solid*) and calculated (*hollow*) half-lives of NTO and DNAN as a function of temperature in aqueous solutions exposed to simulated sunlight [41]
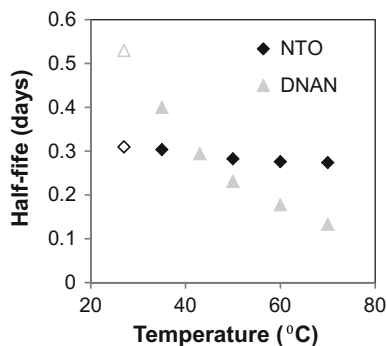
Fig. 13 Plot showing the relationship between NTO concentration and pH for indoor drip samples and outdoor samples [15]
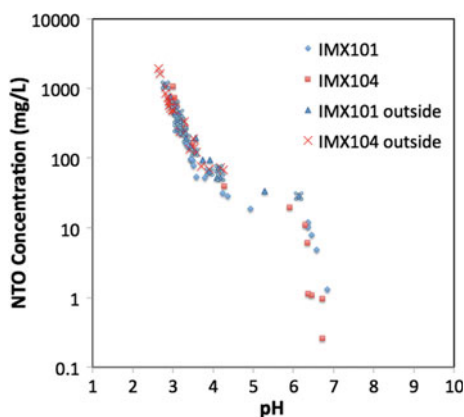
Studies to determine photo-transformation products that form on the surface of IM formulations or on solid pieces of DNAN, as well as experiments under different climatic conditions are underway. Evidence that IM particle surfaces photo-transform include color changes of the outdoor IM pieces (Figs. 6 and 7), the presence of unknown peaks in their HPLC chromatographs (Fig. 12b), and the absence of unknown peaks and good mass balances (100 ± 5%) in the indoor drip tests [16]. Some of these photo-produced compounds color the water samples and, therefore, are soluble.

3.5 PH of the IM Solutions

NTO is known to be acidic in solution $pK_a = 3.8$ [42, 43], and pH measurements of both the drip and the outdoor water samples show how pH changed during dissolution of the particle (Fig. 13). For the IMX-101 drip samples pH values were initially in the low 3 range and increased to neutral as the NTO concentration decreased to 10 mg L^{-1}. The pH of the IMX-104 samples showed a similar trend

with the difference being that, because IMX-104 contains proportionally more NTO than does IMX-101, the concentrations were higher and the pH levels lower for the first few IMX-104 samples. Figure 13 shows that there is a good correlation between NTO concentration and pH values between 2 and 5. At NTO concentrations below 20 mg L^{-1}, the pH is between 4 and 6; and at NTO concentrations below 10 mg L^{-1}, the pH of the solution is close to neutral. The color of the solution was also found to correlate with the NTO concentration—the most yellow colored solutions had the highest NTO concentrations and the lowest pH values. This property has been used to estimate concentration [44].

4 Physiochemical Properties of Insensitive Munitions Formulations

Once in solution, IM constituents and their transformation products experience reactive transport through the soil. En route to ground water, they can undergo irreversible and reversible adsorption by different mineral and organic phases in the soil, transformation, volatilization, and bio-uptake. The importance of each of these processes for the fate of a compound can be evaluated using the octanol-water partition coefficients (K_{ow}), acid dissociation constant (pK_a), Henry's Law constant (K_H), the one-electron standard reduction potential (E_m), the first-order transformation rate constant (k), linear (K_d) or Freundlich (K_f) soil adsorption coefficients, and soil organic carbon absorption coefficients (K_{OC}), among others. While some of these parameters are specific to the individual soil and depend on soil conditions (K_d, k, and partially K_{OC}), others are a function of the compounds' structure only but are linked to its environmental behavior (solubility, K_{ow}, $K_{H,}$ pK_a, and E_m). Table 5 provides values for some of these parameters for compounds in IM and HE formulations.

The octanol–water partition coefficient is a measure of the tendency of the chemical to bio-accumulate and an indicator of its affinity for soil organic matter. Relatively low reported K_{ow} values (Table 5) indicate that these compounds are not strongly adsorbed by organic matter in soils through non-polar interactions. However, they can still experience specific sorption to soil organic matter, as has been shown for TNT and the DNTs (2,4- and 2,6-dinitrotoluene) [45, 46]. Based on the K_{ow} values, one would expect NTO to be more mobile than DNAN and to exhibit similar environmental behaviors to RDX.

Unlike most other explosives, which are polar but non-ionic compounds, NTO is an acid with pK_a of 3.7–3.76 [42, 43] and will be negatively charged at environmentally relevant pHs [47]. As both organic and mineral soil surfaces tend to have a net negative charge, NTO should have a low affinity for soils and a greater mobility in the environment. Relatively low volatility (ability to transfer from an aqueous phase to a gas phase) as measured by Henry's constants (log K_H of −3.25 to −4.40 for DNAN and −11.38 for NTO, [48], indicates that transport in a gas phase will not be important.

Table 5 Environmentally relevant chemical and physical properties, solubility at 25 °C, octanol-water partition coefficient (K_{ow}), acid dissociation constant (pKa), Henry's Law constant (K_H), one-electron standard reduction potentials (E_m), and soil organic carbon adsorption coefficient (K_{oc}) for DNAN, NTO, NQ, RDX, and TNT

Property	DNAN	NTO	NQ	RDX	TNT
Solubility (mg L^{-1})	276.2[a] [21], 213[a] [37],	16,642.0[c] [52]	2600[a] [25]	59.9[a] [53]	100.5[a] [53]
Log K_{ow}	1.58[a] [37], 1.64[a] [48], 1.70–1.92[b] [48]	0.37–1.03[b] [48]	−0.89 to 0.156 [54]	0.81–0.87 [55]	1.6–1.84 [55]
pKa		3.76[a] [47]	12.8[b] [25]		
Log K_H	−3.25 to −4.40[b] [48]	−11.38[b] [47]	−5.15[a] [25]	−10.71[b] [53]	−7.96[b] [53]
E_m (V)	−0.40[a] [49]			−0.55[a] [49]	−0.30[a] [49]
Log K_{oc}	2.2[a] [56], 2.2[b] [57]	1.1[a] [58], 2.1[b] [57]	1.3[a] [59]	2.3 [53]	3.2 [53]

[a]Measured; [b]Estimated; [c]Interpolated from measured values

One-electron standard reduction potential (E_m) is a measure of how easily nitro groups in these compounds reduce to amino groups [49], a common first step in transforming many explosive compounds. Boparai et al. [50] observed faster reduction for explosives having more positive one-electron reduction potentials. Measured electron standard reduction potential for DNAN (−0.40 V) is similar to 2,4-DNT, which is readily reduced in soil environments. Note that transformation products of the compound can have different environmental and toxicity properties than the original contaminant so they are important to identify and study.

5   Soil Interactions

While solubility, K_{ow}, K_H, pK_a, and E_m can be measured independently and used to predict environmental behavior of a contaminant, K_d, k, and K_{OC} need to be measured for soils found at specific locations in order to predict the fate and transport of the IM compounds at those locations. Alternatively these parameters can be measured for a selection of soils and then related to soil properties to extend predictions to other locations and soils.

The soil adsorption, or partitioning, coefficient, K_d, quantifies the absorption of energetics onto soil surfaces. In particular, organic matter, phyllosilicate clays, and iron and aluminum oxides and hydroxides adsorb organic compounds due to their high surface areas [51]. As values of K_d increase, the chemical resides mostly on soil surfaces and little is transported in the moving pore water. Usually, most of the adsorption of organic contaminants in soils can be attributed to soil organic carbon, and K_d values are normalized to soil organic carbon content, described by the soil organic carbon adsorption coefficient (K_{OC}). This parameter can be either derived

from K_{ow} or measured for the energetic in a particular soil, or set of soils. The obtained coefficient can then be used to calculate K_ds and predict the energetic's adsorption to other soils using their carbon contents. For compounds that are adsorbed mostly to organic matter in the soils through non-polar (hydrophobic) interactions K_{OC} can be a good estimate of a compound's adsorption across a range of soil environments.

However, organic matter is not the only soil component that can affect adsorption of energetics in soils. Studies using mineral soil components, phyllosilicate clays and iron and manganese oxides [60], indicated that similarly to TNT [61] DNAN is strongly adsorbed by phyllosilicate clays. The types of cations present on exchange sites in the clays influence the amount of adsorption, with K^+ resulting in the largest adsorption among the cations commonly present in soils. The mechanism of adsorption is based on the interaction between exchangeable cations and nitro-groups of DNAN. DNAN was not adsorbed by either iron or manganese oxides. NTO, on the other hand, experienced negative adsorption (repulsion) by phyllosilicates, as both are negatively charged at environmentally relevant pHs. NTO was strongly adsorbed by birnessite, a manganese oxide, which is positively charged.

Soil adsorption coefficients are measured using kinetic and equilibrium batch soil sorption experiments [62]. In these experiments, soils are mixed with solutions of NTO or DNAN and allowed to equilibrate for a predetermined amount of time. The soil is then separated from the solution and the supernatant analyzed to determine the amount of NTO or DNAN remaining in solution.

Transformation rates (k) of organic compounds in soils are influenced by both inherent soil properties and current soil conditions and therefore are more difficult to extrapolate to different environments and soils. Organic compound transformation is usually microbially driven, though there is some evidence of abiotic transformation catalyzed by soil minerals [60]. During microbial transformation, organic contaminants are either used as a source of energy by the microorganisms or co-metabolized by them, with other sources of carbon fueling their growth. Because of this, microbial transformation can be influenced by amount of the target compound (if it is metabolized) as well as by availability of labile organic carbon (if it is co-metabolized). At the same time, organic contaminants can also be toxic to the soil microorganisms [5, 63], suppressing their growth and decreasing transformation. In addition, since transformation of nitrated compounds commonly involves nitro-group reduction to amino-group, it is also very sensitive to redox state of the soil, which in turn is influenced by soil saturation and amount of available carbon [64]. Because of the factors described above, laboratory estimates of transformation rates (k) are useful for comparisons between different soils or between studied compounds but cannot serve as a reliable estimate of the field transformation rates [56].

Mark et al. [58] and Arthur et al. [56] tested soils collected on military ranges across the United States (Fig. 14). The soils belonged to multiple soil orders, including Entisols, Inceptisols, Mollisols, Aridisols, and Ultisols. Table 6 summarizes the physical and chemical properties for the 11 soils selected for these studies, as well as several other studies that examined NTO and DNAN interaction

Fig. 14 Soils collected from these locations were used for the insensitive munitions batch and column studies by Mark et al. [54] and Arthur et al. [52]

with soils. Soils used by Mark et al. [58] and Arthur et al. [56] had a wide range of OC concentrations (0.34–2.28%), soil pH (4.23–8.00), cation exchange capacity (CEC) (2.9–21.4 cmol kg^{-1}); and particle sizes (loamy sand to clay loam). Soils also varied in the mineral composition of the clay fraction [58].

5.1 Batch Soil Adsorption Studies

5.1.1 NTO

Mark et al. [58] observed that NTO adsorbed very weakly to the studied soils as can be expected for a negatively charged compound in a matrix that also possesses a net negative charge. The determined K_d values were less than 1 cm^3 g^{-1} (Table 6). For most soils, both Freundlich and linear adsorption isotherms described the observed adsorption well (Fig. 15a). Freundlich isotherms usually resulted in a slightly better fit (Table 6) but the Freundlich parameter n was not significantly different from one for the majority of the soils indicating a linear isotherm. When n was significant it was smaller than one [58] indicating a lower affinity for soils at higher NTO concentrations.

Soil pH was the strongest indicator of NTO soil adsorption (Fig. 15b). There was a highly significant negative relationship between linear adsorption coefficients and soil pH. There was no relationship between K_d values and OC, clay, or specific

Table 6 Measured physical and chemical properties of soils used in soil interaction experiments and fate and transport parameters for NTO and DNAN determined in these soils: Freundlich adsorption parameters, K_f and n; soil adsorption coefficient, K_d; log of adsorption coefficient normalized to fraction of OC in soils, log K_{OC}; transformation rate constant, k; half-life, $t_{1/2}$; and R^2 values for linear regressions used to determine these parameters

Soil	Texture	Clay %	pH[a]	OC[c]%	CEC[d] (cmol_c kg^{-1})		K_f	n	R^2	K_d (cm^3 g^{-1})	R^2	Log K_{oc} (cm^3 g^{-1})	k (h^{-1})	$t_{1/2}$ (days)	R^2	Reference
Catlin	Silt loam	25.6	7.31	5.28	21.4	NTO	0.21	1.03	0.94	0.21	0.92	0.6	0.0221	1.3	0.84	[2]
						DNAN	34	0.62	0.98	5.95	0.92	2.1	0.0047	6.1	0.88	[56]
Fort Harrison	Sandy loam	8.7	6.67	3.88	18	NTO	0.27	1.07	0.98	0.35	0.95	1.0	0.0021	13.8	0.98	[2]
						DNAN	13.86	0.77	0.9	6.32	0.93	2.2	0.001	28.9	0.45	[56]
Arnold AFB	Silt loam	11.4	6.66	2.68	8.7	NTO	0.58	0.86	0.98	0.34	0.94	1.1	0.0044	6.6	0.94	[2]
						DNAN	14.4	0.68	0.93	3.39	0.78	2.1	0.0022	13.1	0.92	[56]
Plymouth	Loamy sand	4.4	4.23	2.45	6.8	NTO	0.82	0.89	0.99	0.5	0.96	1.3	0.0043	6.7	0.97	[2]
						DNAN	10.05	0.83	0.98	4.38	0.94	2.3	0.007	4.1	0.51	[56]
Camp Butner	Sandy loam	7.7	6.69	2.42	6.1	NTO	0.74	0.54	0.77	0.12	0.72	0.7	0.0021	13.8	0.98	[2]
						DNAN	15.35	0.56	0.91	2.05	0.92	1.9	0.0018	16.0	0.67	[56]
Limestone	Sandy loam	11.2	7.54	1.99	13	NTO	0.33	0.88	0.92	0.21	0.92	1.0	0.0123	2.3	0.6	[2]
						DNAN	10.75	0.77	0.96	4.96	0.92	2.4	0.0019	15.2	0.78	[56]
Sassafras	Loam	16.4	4.4	1.3	7.9	NTO	0.9	0.86	0.99	0.48	0.96	1.6	0.008	3.6	0.99	[2]
						DNAN	2.26	0.97	0.85	1.89	0.72	2.4	0.0013	22.2	0.54	[56]
Camp Gruber	Clay loam	32.3	5.39	0.83	14.3	NTO	0.54	0.99	1	0.51	0.99	1.8	0.0025	11.6	0.98	[2]
						DNAN	7.62	0.72	0.84	1.99	0.91	2.4	0.0073	4.0	0.29	[56]
Camp Guernsey	Loam	4.1	8.21	0.77	2.9	NTO	0.06	0.48	0.18	0.02	0.21	0.4	0.0004	72.2	0.75	[2]
						DNAN	1.72	0.85	0.93	0.93	0.97	2.1	0.0041	7.0	0.85	[56]
Florence MR	Loam	26.8	8	0.45	12.2	NTO	0.09	0.77	0.55	0.06	0.57	1.1	0.0005	57.8	0.91	[2]
						DNAN	6.59	0.74	0.98	1.91	0.94	2.6	0.0007	41.3	0.35	[56]
Camp swift	Sandy clay loam	23.7	7.83	0.34	6.5	NTO	0.1	0.84	0.92	0.04	0.59	1.1	0.0009	32.1	0.93	[2]
						DNAN	1.27	0.84	0.7	0.6	0.84	2.2	0.0006	48.1	0.96	[56]
Petawawa		44.1[e]	4.9	2.5	<10	DNAN				9.1		2.7				[37]
Topsoil		0.4	6.1	34	35.0	DNAN				73		2.3				[37]

(continued)

Table 6 (continued)

Soil	Texture	Clay %	pH[a]	OC[c]%	CEC[d] (cmol_c kg^{-1})		K_f	n	R^2	K_d (cm^3 g^{-1})	R^2	Log K_{oc} (cm^3 g^{-1})	k (h^{-1})	$t_{1/2}$ (days)	R^2	Reference
DRDC-09		1.5	6.7	2.08	13.2	NTO				<0.1						[65]
						DNAN				2.27		2.0				[65]
Sandy clay loam	Sandy clay loam	21	6.6	1	14	NTO	1.39	1.33								[19]
						DNAN	0.68	1.28								[19]
Sand	Sand	0.03				NTO	0.34	1.04								[19]
						DNAN	0.17	1.18								[19]

[a]In 1:1 soil:water; [b]*OC* Organic carbon; [c]*CEC* Cation Exchange Capacity; [d]Includes silt

(a)

y = 0.48x
$R^2 = 0.99$

y = 0.21x
$R^2 = 0.92$

y = 0.04x
$R^2 = 0.61$

Soil NTO, mg kg^{-1}

Solution NTO, mg L^{-1}

(b)

y = -0.12x + 1.07
$R^2 = 0.82$

K_d (cm^3 g^{-1})

pH
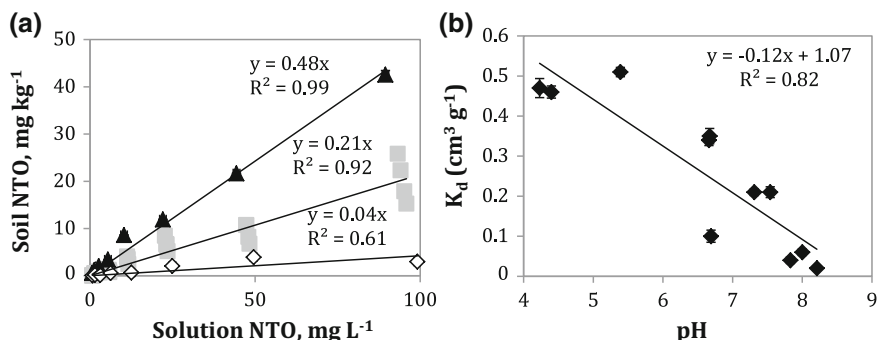
Fig. 15 a Adsorption isotherms for NTO in Sassafras, Catlin, and Camp Swift soil (listed highest to lowest adsorption); **b** Measured NTO adsorption coefficients (K_d) plotted against soil pH. $P = 0.00011$ [54]

surface area (SSA). The K_f values had similar but slightly weaker ($R^2 = 0.7818$, $P = 0.00030$) negative linear relationship with pH.

For Catlin soil that has a high pH and a high OC content, NTO was absorbed about 10 times less than RDX, K_d of 0.21 versus 2.03 cm^3 g^{-1} [51], while for Plymouth soil (low pH, less OC) the difference was smaller, 0.50 versus 0.65 cm^3 g^{-1} [14]. These results indicate that RDX and NTO are adsorbed through different mechanisms and that OC content is not a good predictor of NTO adsorption. The log K_{OC} for NTO in tested soils (1.06 ± 0.40 cm^3 g^{-1}) was significantly smaller compared to the literature value for RDX (2.26 ± 0.56 cm^3 g^{-1}) [53]. The K_{OC} values also had a higher percent standard deviation (102.7%) than K_d values from which they were calculated (72.8%) indicating that normalizing to OC did not decrease the variability.

The low NTO adsorption measured by Mark et al. [58] agreed with measurements by Hawari et al. [65] and Richard and Weidhaas [33]. We suggest that NTO adsorption may be either attributed to limited positive sites in the soils, such as birnessite or amino-groups in organic matter, or to interactions between non-charged NTO molecules at low pHs and non-charged soil sites. Linear isotherms support the second mechanism for NTO adsorption.

NTO also transformed in the soils [58]. Mass balance calculations (Fig. 16) indicated that after 24 h of equilibration there was little or no difference in NTO mass recovered between sterilized and non-sterilized soils. After 120 h, however, non-sterilized samples lost more NTO, indicating removal by microorganisms. In high OC soil (Catlin) the majority of NTO was transformed. Even in sterilized Catlin soil about 50% of NTO was lost from the solution in 120 h, probably due to abiotic transformation. This finding indicates a strong potential for natural attenuation.

Microbial transformation studies of NTO in soils show nitro-reduction followed by oxidative ring cleavage of the primary amine, 5-amino-1,2,4-triazol-3-one
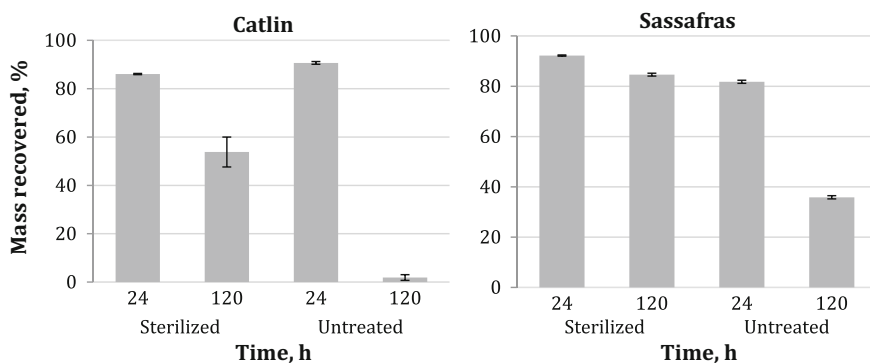
Fig. 16 Batch experiments for Sassafras and Catlin soils comparing mass (%) associated with solution and soil for sterilized (autoclaved) versus untreated soils. Soils and NTO solutions were reacted for 24 and 120 h. Error bars equal one standard error of the mean [54]

Fig. 17 Correlation between measured NTO transformation rate constants (k) and soil OC. $P = 0.02250$ [54]
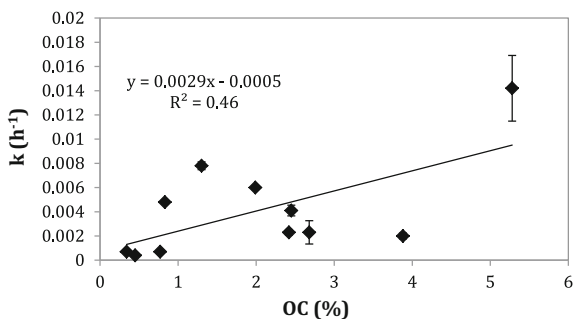
(ATO) forming a number of inorganic compounds [66, 7]. Mn oxide (birnessite) can abiotically oxidize ATO [60].

First-order rate coefficient estimates for transformation reactions range between $0.0004 \ h^{-1}$ in Camp Guernsey and $0.0221 \ h^{-1}$ in Catlin soil [58]. Measured transformation rates were lower for soils with less OC, such as Camp Guernsey, Florence MR, and Camp Swift. There was a positive relationship between the percent OC present in the soil and the measured transformation rate constant k (probability, $P = 0.02$), however, R^2 was low at 0.46 (Fig. 17). Other soil parameters, such as clay content, pH, and SSA, poorly correlated with k. The NTO transformation rate constant in Plymouth soil, $0.0043 \ h^{-1}$, was about three times smaller than one measured previously for RDX in the same soil ($0.013 \ h^{-1}$) [14].

5.1.2 DNAN

Unlike NTO, DNAN adsorbes to the soils [56] indicating that natural attenuation may be an important mechanism for DNAN remediation. For all studied soils, the
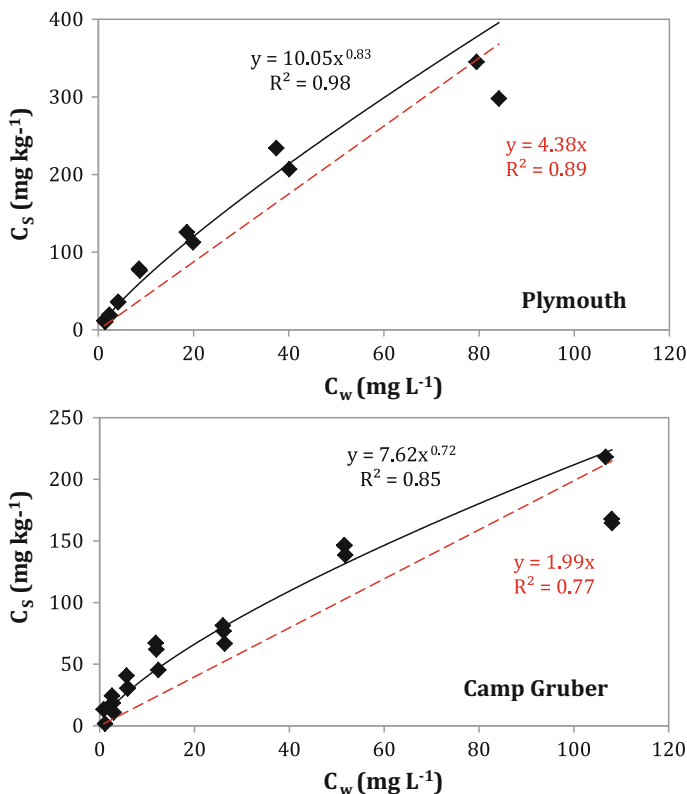
Fig. 18 Adsorption isotherms calculated for DNAN in Plymouth and Camp Gruber soils. The *red dashed line* indicates the linear adsorption isotherm fit to the measured adsorption data (equation is in *red*) while the *solid black line* is a fit of the Freundlich isotherm with the equation presented in *black* [41]

Freundlich isotherm resulted in a highly significant fit to the data (Table 6; Fig. 18). The mean value of the Freundlich parameter, *n,* across all the soils was equal to 0.76 ± 0.21. The 95% confidence intervals of n estimates overlapped for the majority of the soils, indicating that they were not significantly different from each other. For three soils, Sassafras, Camp Guernsey and Camp Swift, n was not significantly different from 1 (resulting in a linear isotherm).

Linear regressions for the isotherms were also highly significant (Table 6). For the majority of soils, a Freundlich isotherm described DNAN adsorption the best, but for four soils, Fort Harrison, Sassafras, Camp Guernsey, and Camp Swift, a linear isotherm resulted in a better fit to the data (Fig. 18). Normalizing estimated K_d values to OC content in the soil (K_{OC}) resulted in a decrease in the percent standard deviation of the estimates from 61 to 49%. The mean log K_{OC} value was 2.24 ± 0.20 similar to 2.33 ± 0.35 measured by Hawari et al. [37, 65].

(a)

$y = 1.12x + 0.842$
$R^2 = 0.74$

K_d (L kg^{-1})

OC (%)

(b)

$y = 0.2622x + 0.3239$
$R^2 = 0.54$

CEC (cmol kg^{-1})
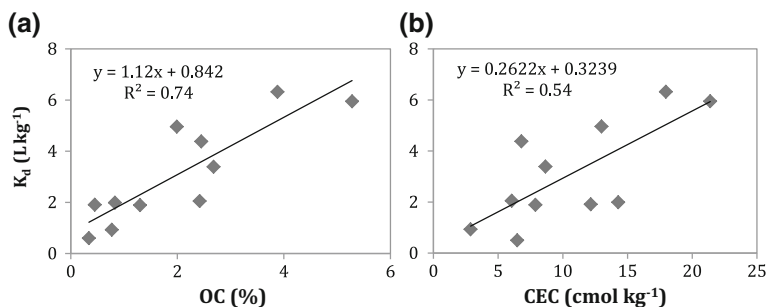
Fig. 19 Correlation between measured DNAN adsorptions coefficients (K_ds) and percent organic carbon in soil (OC) ($P = 0.00061$) (**a**) and cation exchange capacity (CEC) ($P = 0.0095$) (**b**) [52]

The determined DNAN adsorption coefficients, K_ds, resulted in highly significant positive relationships with percent OC in the soil (Fig. 19a) and CEC (Fig. 19b). Similarly significant linear relationships were observed between K_fs and OC and CEC [56]. No other measured soil properties, such as clay content, pH, or SSA, correlated with K_d or K_f values.

Lower DNAN K_{ow} and K_{OC} values (Table 5) indicate that it would have less affinity for soils than TNT. Comparing DNAN with TNT adsorption coefficients for Catlin and Plymouth soils [52] confirmed this trend for Catlin soil: K_d values were higher for TNT than DNAN (17.9 vs. 5.95) [51], though Freundlich parameters were similar for the two compounds ($K_f = 34.00$, n = 0.62 for DNAN and $K_f = 32.67$, n = 0.60 for TNT). However, in Plymouth soil DNAN adsorbed more strongly than TNT (K_d of 4.38 cm^3 g^{-1} for DNAN and 0.63–1.6 cm^3 g^{-1} for TNT, depending on the method used) [14].

Mechanisms of DNAN adsorption in soils likely include adsorption to phyllosilicate clays and interactions with organic matter. Evidence of the latter comes from a strong correlation between OC and adsorption coefficients (Fig. 19a) that indicates OC and K_ds are linked [56], while the former is supported by direct experiments with clays [60] and correlations between cation exchange capacity (CEC) and DNAN adsorption coefficients (Fig. 19b) [56]. We suggest that DNAN interacts with soil organic matter through hydrophobic partitioning and specific adsorption, as is seen for TNT [67]. The non-linear shape of the adsorption isotherms supports the contribution of specific adsorption. In addition to direct DNAN reactions with soils, DNAN reduction products can adsorb irreversibly to soil organic matter, similar to amino-products of TNT transformation [37].

To study the effect of microbial transformation, two sterilized and unsterilized soils with different OC concentrations were equilibrated with DNAN for 24 and 120 h. For the sterilized Sassafras soil the 24 and 120-h recoveries were similar and close to 100% (Fig. 20) [56]. For the unsterilized Sassafras soil the 120-h recovery was lower than when sterilized. These results indicate that the significant mass loss observed for the unsterilized Sassafras soil is due to biotic transformation, with minor contributions by abiotic transformation or irreversible adsorption; biotic
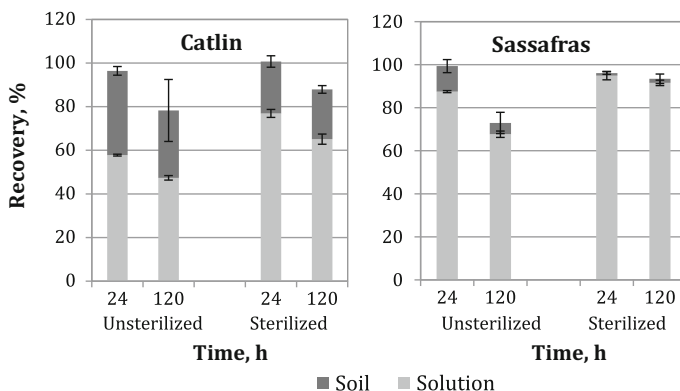
Fig. 20 Mass balance of DNAN in unsterilized and sterilized Catlin (5.28% OC) and Sassafras (1.30% OC) soils for 24 and 120 h of contact. Error bars equal confidence interval of the mean [56]

transformation was also seen in soils by Olivares et al. [8]. Conversely, for the sterilized Catlin soil, the 120-h recovery is significantly lower than the 24-hr recovery, indicating a contribution of abiotic transformation or irreversible adsorption or both.

The transformation rate constant, k, ranged between 0.0006 and 0.0073 h^{-1} for Camp Swift and Camp Gruber soils, resectively [56]. Although k appears to increase with OC, the trend is not statistically significant ($P = 0.78101$). This study found that other soil parameters, such as pH, clay content, and SSA, did not correlate with k. No known products of DNAN tranformation were measured in the solutions.

DNAN transformation observed in batch studies [56] was significantly slower than observed for TNT. For Plymouth soil, the TNT transformation rate constant was 0.21 h^{-1} [14] while the DNAN constant was 0.0070 h^{-1}. The environmental behaviors of NQ and RDX are described in Dontsova and Taylor [13].

5.2 Solution Transport for NTO and DNAN and HYDRUS-1D Modeling Results

HYDRUS-1D is a widely used numerical model that simulates variably saturated water flow and solute transport in porous media. We have used the HYDRUS-1D model to analyze breakthrough curves of a nonreactive tracer to determine the physical parameters characterizing the column experiments, and then, with fixed physical parameters, to analyze breakthrough curves of reactive compounds to determine the chemical and reaction processes involved. We compare the reaction parameters determined from the model to the same parameters independently measured in soil batch studies and drip tests. Agreement between the two sets of values indicates how well the determined relationships characterize the release and transport of IM components in soils.
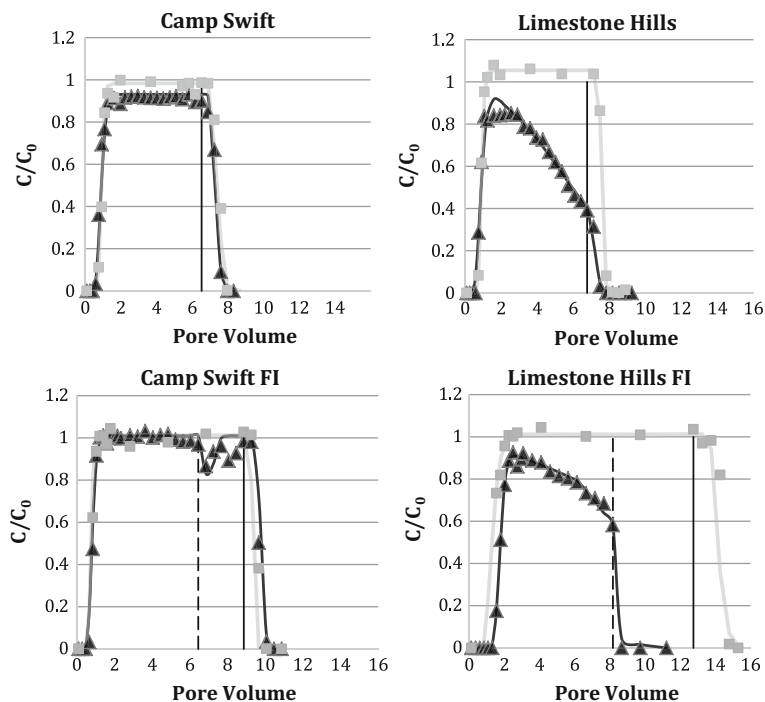
Fig. 21 Measured (*points*) and HYDRUS-simulated (*lines*) breakthrough curves for NTO (*black*) and Br– tracer (*grey*) in Camp Swift and Limestone Hills soils under conditions of continuous flow and flow interruption (FI). The *thin dashed black vertical line* shows the start of 24 h when the flow was interrupted. The *thin solid black line* indicates the time when the solution was changed back to 0.005 M CaCl$_2$ to observe the desorption phase of the isotherm [64]

To resolve non-equilibrium processes, column transport studies were conducted with continuous flow and 24-h flow interruption. In these experiments NTO or DNAN was added to the column with 0.005 M CaBr$_2$, where Br$^-$ served as a conservative tracer. After flow interruption the solution was switched to only 0.005 M CaCl$_2$ to observe desorption of NTO and DNAN from soils. A subset of the soils used in the batch experiments was used for the column tests. NTO had low retardation (Figs. 21 and 22; Table 7), in agreement with low K_ds measured in batch experiments, but experienced transformation in the soils. First order transformation kinetics (manifested by constant effluent concentration during steady-state conditions) was observed for half of the studied soils (Sassafras (Fig. 22), Camp Guernsey, Florence MR, and Camp Swift (Fig. 21)) in agreement with batch experiments. Transformation rate constants, however, were higher than determined in batch studies [58]. In these soils, flow interruption decreased effluent concentration, but concentrations recovered after the flow was restarted (Fig. 21, Camp Swift).
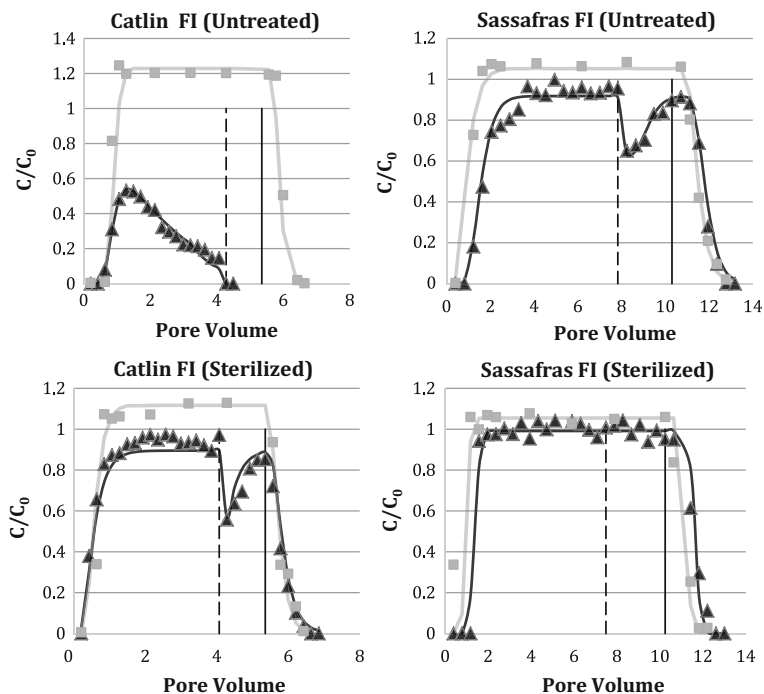
Fig. 22 Measured (*points*) and HYDRUS-simulated (*lines*) breakthrough curves for NTO (*black*) and Br– tracer (*grey*) in untreated and autoclaved Catlin and Sassafras soils. *Thin dashed black vertical line* indicates timing of 24-h flow interruption. *Thin solid black vertical line* indicates time when solution was changed back to 0.005 M CaCl₂ to observe desorption phase of the isotherm (modified from [64])

For the other soils, Catlin (Fig. 22), Arnold AFB, Camp Butner, and Limestone Hills (Fig. 21), effluent concentration decreased with time, indicating a change in the transformation rate constant. It was determined that Monod kinetics successfully described breakthrough curves for these soils. For these soils, when flow was interrupted concentrations decreased below the detection limit and did not recover when flow was restarted. This behavior was associated with soils that had higher OC contents than soils that had 1st rate kinetics of transformation (Table 7). To test if the pattern could be explained by microbial activity in the soils, Mark et al. [64] sterilized two soils, Catlin with high OC content (Table 5) and decreasing eluent concentrations with time, and Sassafras with lower OC and steady-state concentrations of NTO in the effluent. As a result of sterilization, Catin soil also had steady-state concentrations of NTO in the effluent (Fig. 22) confirming that microbial activity was responsible for the difference in patterns.

Fast transformation of NTO could result if reducing conditions develop in the soil. This could occur if microbial activity increased due to organic matter and water flow in the soils. The consumption of oxygen by microorganisms would

Table 7 NTO fate and transport parameters determined by HYDRUS-1D, linear adsorption coefficients, K_d, 1st order transformation rate constants, k, and initial Monod transformation rate, with average rate shown in parentheses

Soil	K_d (cm^3 g^{-1})		k (h^{-1})		Monod transformation rate (h^{-1})		R^2
	Estimate	95% CI	Estimate	95% CI	Estimate	95% CI	
Catlin	0.15	0.04			0.058 (0.123)	0.016	0.97
Catlin FI	0.04	0.04			0.046 (0.133)	0.017	0.96
Arnold AFB	0.17	0.02			0.072 (0.121)	0.008	0.99
Arnold AFB FI	0.13	0.02			0.067 (0.133)	0.010	0.98
Camp Butner	0.12	0.01			0.207 (0.259)	0.023	0.99
Camp Butner FI	0.06	0.01			0.100 (0.183)	0.011	0.99
Limestone Hills	0.00	0.01			0.038 (0.154)	0.011	0.99
Limestone Hills FI	0.15	0.01			0.034 (0.186)	0.009	0.99
Sassafras	0.05	0.01	0.100	0.008			0.99
Sassafras FI	0.40	0.32	0.076	0.064			0.96
Camp Guernsey	0.03	0.01	0.009	0.009			0.98
Camp Guernsey FI	0.05	0.01	0.064	0.010			0.98
Florence MR	0.03	0.01	0.065	0.012			0.98
Florence MR FI	0.04	0.01	0.041	0.003			0.97
Camp Swift	0.00	0.00	0.040	0.008			0.98
Camp Swift FI	0.04	0.01	0.009	0.004			0.99

Soils are listed in order of decreasing OC% (modified from [64]. FI = flow interruption
CI = 95% confidence interval

decrease the redox potential in the solution causing NTO to be reduced to ATO. In turn, Linker et al. [60] showed that ATO can be oxidized by Mn oxide to form a variety of organic and inorganic products. Thus, NTO could be completely attenuated in high OC soils under field conditions.

Similarly to NTO, DNAN experienced higher transformation rates in column transport than in batch experiments (Fig. 23) [56]. In addition, while no DNAN transformation products were detected in batch experiments, both 2-methoxy-5-nitroanisole and 4-methoxy-3-nitroanisole were measured in the column effluent. Even in the two low OC soils used in column expreriments (Camp Swift and Camp Gruensey) DNAN was significantly retarded and transformed.

5.3 Dissolution and Transport of IM Formulations

Dissolution and transport studies for IMX-101 and IMX-104 were performed using Camp Swift and Camp Guernsey soils [41]. These soils were selected because of
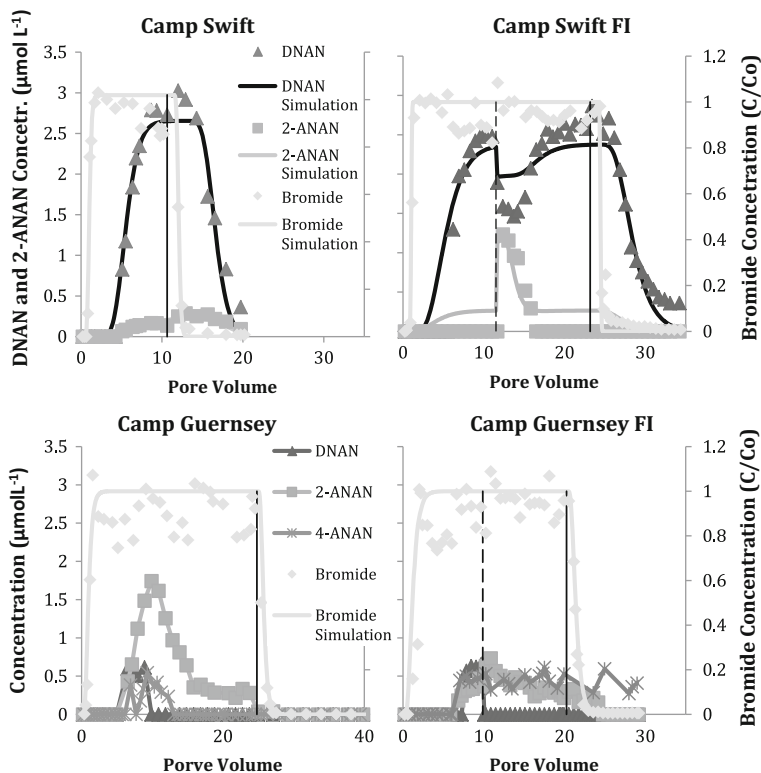
Fig. 23 Breakthrough curves for DNAN, 2-methoxy-5-nitroaniline (2-ANAN), 4-methoxy-3-nitroaniline (4-ANAN), and Br^{-1} tracer in Camp Swift and Camp Guernsey soils for continuous flow and flow interruption (FI). DNAN inflow concentration was 2.87 and 2.64 $\mu mol\ L^{-1}$ in Camp Swift, and 2.71 and 2.78 $\mu mol\ L^{-1}$ in Camp Guernsey respectively for continuous and interrupted flow experiments. *Vertical dashed line* indicates time of flow interruption and *solid line* indicates time when input solution was switched back to 0.005 M CaCl$_2$ [56]

their low organic matter content that provides a conservative estimate for IM constituents' attenuation in soils (Table 6). IM particles were placed on the soil surface and subjected to water flow until steady-state concentrations of IM constituents were measured in the effluent; then particles were removed and water flow continued to observe IM desorption.

Breakthrough curves were observed for all IMX-101 components. In addition, 2-methoxy-5-nitroaniline, a DNAN transformation product, was detected in the effluent at concentrations about 2 orders of magnitude lower than DNAN. Dissolution of all IM components was successfully simulated in HYDRUS-1D given: that the maximum dissolution occurred right after the initial exposure of IM101 particles to the flow and; that the dissolution rate decreased at an exponential rate until a steady-state rate was reached. This model was previously used to
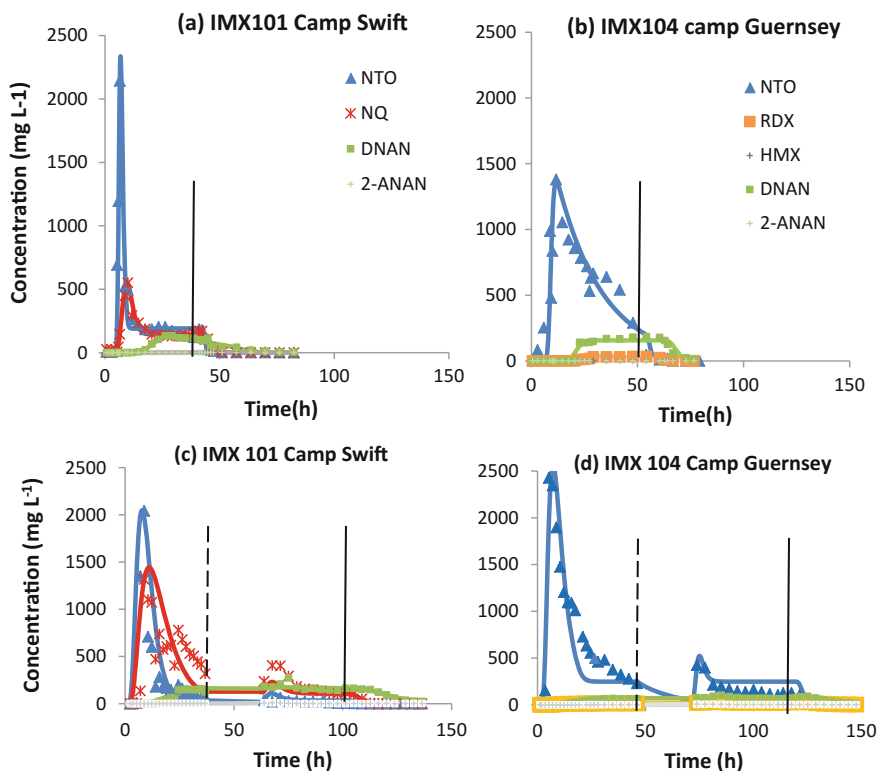
Fig. 24 Measured (*points*) and HYDRUS-1D simulated (*lines*) breakthrough curves for NTO, NQ, RDX, HMX, DNAN, and DNAN's transformation product, 2-methoxy-5-nitroaniline (2-ANAN). **a** IMX-101 particle dissolved on Camp Swift soil. **b** IMX-104 particles on Camp Gruensey soil. **c, d** Corresponding flow interruption experiments. *Vertical dashed line* indicates time of flow interruption and solid line indicates time when input solution was switched back to 0.005 M CaCl$_2$ and IM particle removed

describe dissolution of propellants from nitrocellulose matrices [59] and can be applied to melt-cast IM particles due to the large difference in solubility between the DNAN matrix and the crystal constituents of the IM formulations.

The shape of the breakthrough curves and the measured concentrations varied appreciably between IM constituents (Fig. 24a). NTO had the highest initial effluent concentrations despite representing only about 20% of the total IMX-101 mass. This agrees with NTO results from drip and outdoor studies [16, 32]. Although NTO concentrations were initially very high, they quickly decreased to smaller steady-state effluent concentrations. For NQ, initial concentrations were smaller than for NTO (despite higher content of NQ in IMX-101 but in agreement with lower NQ solubility), and transition to steady state was slower. For DNAN, effluent concentrations were stable over time indicating a near-constant dissolution rate. The DNAN concentrations were much smaller than peak concentrations for

either NTO or NQ but similar to the steady-state concentrations of these compounds.

The behavior of NTO, DNAN, and NQ dissolving from IM particles and transported to soils was consistent with previously measured fate and transport parameters [56, 58]. NTO experienced minimal retardation in the soils and was the first compound to break through. Early NTO breakthrough is consistent with low measured adsorption coefficients for both studied soils (0.02 and 0.04 cm^3 g^{-1} for Camp Guernsey and Camp Swift, respectively). Nitroguanidine, similarly to NTO, is a relatively inert compound in soil environments. Nitroguanidine K_d values for Sassafras, Plymouth, and Catlin soils were 0.60, 0.44, and 0.24 cm^3 g^{-1} [59] compared to 0.48, 0.50, and 0.21 cm^3 g^{-1} measured for NTO in the same soils. Breakthrough curves, however, indicated a slightly later arrival of NQ compared to NTO and a delay in desorption, indicating that NQ has a higher affinity for these soils than does NTO. DNAN was the last IM constituent to breakthrough. It also had a corresponding delay in desorption.

For IMX-104 similar trends were observed (Fig. 24b): NTO dissolved 1st, had the highest initial effluent concentrations that decreased sharply over time, and exibited minimal retardation in soils, while DNAN had stable dissolution, lower concentrations, and higher retardation in soils. RDX had lower concentrations than DNAN and experienced intermediate retardation, while HMX eluted at about a 10 times smaller concentrations than RDX and was strongly adsorbed. In interrupted flow experiments there was an increase in NTO concentration after flow resumption, consistent with continued dissolution during flow interruption (Fig. 24c, d).

6 Summary

The solubility of the individual constituents of IM formulations differs by orders of magnitude and produce porous particles as they dissolve. This process increases both the surface areas and the dissolution rates of the particles. Both the dissolution results and the μCT data show that the components in these explosive formulations dissolve sequentially and in the order predicted by their solubility i.e. NTO, NQ and DNAN. We expect the low pH of water containing dissolved NTO and the contaminant mixtures of the effluent to affect microbial communities in ways that are currently unknown.

The good mass balances measured for the laboratory drip tests indicate that the dissolved formulations do not significantly photo- or bio-transform when not exposed to sunlight. Photo-transformation does occur outdoors as evidenced by (1) DNAN changing color and (2) unknown peaks appearing in the HPLC chromatograms of the effluent from outdoor dissolution tests. Although photo-transformation products are present they were found to be small relative to the dissolved DNAN.

Both NTO and DNAN photo-transform when in solution. In pure water, DNAN photo-transformed more than NTO. However, rates were sensitive to solution

chemistry. NTO photo-transformation was enhanced in acidic and basic solutions. NTO photo-transformation rates also increased by a factor of three in the presence of organic matter that commonly occurs in soil solutions and in surface waters. Dissolved organic matter did not affect DNAN photo-transformation. We found the photo-transformation of NTO to be relatively insensitive to temperature between 35 and 70 °C. For DNAN, on the other hand, photo-transformation rates increased with increasing temperature.

Both NTO and DNAN experienced adsorption and transformation in soils. NTO was weakly adsorbed, with adsorption coefficients lower than those measured for RDX, the explosive compound it is replacing, and the explosive that has been found in groundwater beneath training ranges. NTO adsorption was not influenced by organic carbon in the soil but was strongly affected by soil pH. Adsorption decreased as soil pH increased, probably due to changes in protonation (and therefore charge) of both the soil surfaces and NTO. DNAN adsorption was similar to TNT and positively correlated with organic carbon.

Column studies supported batch-determined parameters that indicated increased transformation as soil becomes slightly anaerobic. NTO transformation rates increased with increases in soil organic carbon. NTO had little affinity for soils, making it more mobile in the environment than DNAN, and as it is also more soluble, we can expect it to reach ground water faster. DNAN is easily photo-transformed and adsorbed in the soil, making it less mobile in the environment. The solubility of most IM constituents is higher than that of TNT and RDX, increasing the likelihood that they will reach groundwater.

References

1 Mirecki JE, Porter B, Weiss CA (2006) Environmental transport and fate process descriptors for propellant compounds. U.S. Army Engineer Research and Development Center, Vicksburg, MS

2 Walsh MR, Walsh ME, Ramsey CA, Thiboutot S, Ampleman G, Diaz E, Zufelt JE (2014) Energetic residues from the detonation of IMX-104 insensitive munitions. Propellants, Explos, Pyrotech 39:243–250

3 Olivares CI, Abrell L, Khatiwada R, Chorover J, Sierra-Alvarez R, Field JA (2016) (Bio)transformation of 2,4-dinitroanisole (DNAN) in soils. J Hazard Mater 304:214–221

4 Lee K-Y, Chapman LB, Cobura MD (1987) 3-Nitro-1,2,4-triazol-5-one, a less sensitive explosive. J Energ Mater 5:27–33

5 Fung V, Price D, LeClaire E, Morris J, Tucker N, Carrillo A (2010) Further development and optimization of IM ingredients at Holston Army Ammunition Plant. In: 2010 insensitive munitions and energetic materials technology symposium, Munich, Germany

6 Walsh MR, Walsh ME, Taylor S, Ramsey CA, Ringelberg DB, Zufelt JE, Thiboutot S, Ampleman G, Diaz E (2013) Characterization of PAX-21 insensitive munition detonation residues. Propellants, Explos, Pyrotech 38:399–409

7 Taylor S, Dontsova K, Walsh ME, Walsh MR (2015) Outdoor dissolution of detonation residues of three insensitive munitions (IM) formulations. Chemosphere 134:250–256

8 Rao B, Wang W, Cai Q, Anderson T, Gu B (2013) Photochemical transformation of the insensitive munitions compound 2,4-dinitroanisole. Sci Total Environ 443:692–699

9 Uchimiya M, Gorb L, Isayev O, Qasim MM, Leszczynski J (2010) One-electron standard reduction potentials of nitroaromatic and cyclic nitramine explosives. Environ Pollut 158:3048–3053

10 Walsh MR, Walsh ME, Ramsey CA, Thiboutot S, Ampleman G, Dowden J (2015) Energetic residues from the detonation of IMX101 and IMX-104 munitions. ERDC/CRREL TR-15-3

11 Arthur JD, Mark NW, Taylor S, Šimunek J, Brusseau ML, Dontsova KM (2017) Batch soil adsorption and column transport studies of 2,4-dinitroanisole (DNAN) in soils. J Contam Hydrol 199:14–23

12 Chakka S, Boddu VM, Maloney SW, Damavarapu R (2008) Prediction of physicochemical properties of energetic materials via EPI suite. American Institute of Chemical Engineers Annual Meeting, Philadelphia, PA

13 Wilson A (2007) Explosive ingredients and compositions for the IM M795 In: Artillery ammunition. 2007 insensitive munitions and energetic materials technology symposium, Miami, FL

14 Boddu VM, Abburi K, Maloney SW, Damavarapu R (2008) Thermophysical properties of an insensitive munitions compound, 2,4-dinitroanisole. J Chem Eng Data 53:1120–1125

15 Smith MW, Cliff MD (1999) NTO based explosive formulations: a technology review. Weapons Systems Division, Aeronautical and Maritime Research Laboratory

16 Taylor S, Dontsova K, Bigl S, Richardson C, Lever J, Pitt J, Bradley JP, Walsh M, Šimůnek J (2012) Dissolution rate of propellant energetics from nitrocellulose matrices. Cold Regions Research and Engineering Laboratory, Hanover, NH

17 Monteil-Rivera F, Paquet L, Deschamps S, Balakrishnan V, Beaulieu C, Hawari J (2004) Physico-chemical measurements of CL-20 for environmental applications. Comparison with RDX and HMX. J Chromatogr A 1025:125–132

18 Krzmarzick MJ, Khatiwada R, Olivares CI, Abrell L, Sierra-Alvarez R, Chorover J, Field JA (2015) Biotransformation and degradation of the insensitive munitions compound, 3-nitro-1,2,4-triazol-5-one, by soil bacterial communities. Environ Sci Technol 49:5681–5688

19 Taylor S, Walsh ME, Becher JB, Ringelberg DB, Mannes PZ, Gribble GW (2017) Photo-degradation of 2,4-dinitroanisole (DNAN): an emerging munitions compound. Chemosphere 167:193–203

20 Le Campion L, Vandais A, Ouazzani J (1999) Microbial remediation of NTO in aqueous industrial wastes. FEMS Microbiol Lett 176:197–203

21 Lotufo GR, Biedenbach JM, Sims JG, Chappell P, Stanley JK, Gust KA (2015) Bioaccumulation kinetics of the conventional energetics TNT and RDX relative to insensitive munitions constituents DNAN and NTO in Rana pipiens tadpoles. Environ Toxicol Chem 34 (4):880–886

22 Taylor S, Park E, Bullion K, Dontsova K (2015) Dissolution of three insensitive munitions formulations. Chemosphere 119:342–348

23 Le Campion L, Giannotti C, Ouazzani J (1999) Photocatalytic degradation of 5-nitro-1,2,4-triazol-3-one NTO in aqueous suspention of TiO_2. Comparison with Fenton oxidation. Chemosphere 38:1561–1570

24 Hill FC, Sviatenko LK, Gorb L, Okovytyy SI, Blaustein GS, Leszczynski J (2012) DET M06-2X investigation of alkaline hydrolysis of nitroaromatic compounds. Chemosphere 88:635–643

25 Haag WR, Spanggord R, Mill T, Podoll RT, Chou T-W, Tse DS, Harper JC (1990) Aquatic environmental fate of nitroguanidine. Environ Toxicol Chem 9:1359–1367

26 Salter-Blanc AJ, Bylaska EJ, Ritchie JJ, Tratnyek PG (2013) Mechanisms and kinetics of alkaline hydrolysis of the energetic nitroaromatic compounds 2,4,6-trinitrotoluene (TNT) and 2,4-dinitroanisole (DNAN). Environ Sci Technol 47:6790–6798

27 Haderlein SB, Weissmahr KW, Schwarzenbach RP (1996) Specific adsorption of nitroaromatic explosives and pesticides to clay minerals. Environ Sci Technol 30:612–622

28 Roy WR, Krapac IG, Chou SFJ, Griffin RA (1992) Batch-type procedures for estimating soil adsorption of chemicals. Risk Reduction Engineering Laboratory, Cincinnati, OH, p 100

29 Liang J, Olivares C, Field JA, Sierra-Alvarez R (2013) Microbial toxicity of the insensitive munitions compound, 2,4-dinitroanisole (DNAN), and its aromatic amine metabolites. J Hazard Mater 262:281–287

30 Mark N, Arthur J, Dontsova K, Brusseau M, Taylor S, Šimůnek J (2017) Column transport studies of 3-nitro-1,2,4-triazol-5-one (NTO) in soils. Chemosphere 171:427–434

31 Hawari J, Perreault N, Halasz A, Paquet L, Radovic Z, Manno D, Sunahara GI, Dodard S, Sarrazin M, Thiboutot S, Ampleman G, Brochu S, Diaz E, Gagnon A, Marois A (2012) Environmental fate and ecological impact of NTO, DNAN, NQ, FOX-7, and FOX-12 considered as substitutes in the formulations of less sensitive composite explosives. National Research Council Canada

32 Thorn KA, Pennington JC, Hayes CA (2001) Transformation of TNT in an aerobic compost: Structure and reactivity effects in the covalent binding of aromatic amines to organic matter. Abstr Pap Am Chem Soc 41:628–632

33 Chipen GI, Bokalder RP, Grinstein VY (1966) 1,2,4-triazol-3-one and its nitro and amino derivatives. Chem Heterocycl Compd 2:110–116

34 Mark N, Arthur J, Dontsova K, Brusseau M, Taylor S (2016) Adsorption and attenuation behavior of 3-nitro-1,2,4-triazol-5-one (NTO) in eleven soils. Chemosphere 144:1249–1255

35 Taylor S, Lever JH, Fadden J, Perron N, Packer B (2009) Outdoor weathering and dissolution of TNT and Tritonal. Chemosphere 77:1338–1345

36 Nandi AK, Singh SK, Kunjir GM, Singh J, Kumar A, Pandey RK (2012) Assay of the insensitive high explosive 3-nitro-1,2,4- triazol-5-one (NTO) by acid-base titration. Cent Eur J Energ Mater 2:4–5

37 Taylor S, Lever JH, Bostick B, Walsh MR, Walsh ME, Packer B (2004) Underground UXO: are they a significant source of explosives in soil compared to low- and high- order detonations? ERDC/CRREL technical report TR-04-23

38 Dontsova K, Taylor S, Pesce-Rodriguez R, Brusseau M, Arthur J, Mark N, Walsh M, Lever J, Šimůnek J (2014) Dissolution of NTO, DNAN, and insensitive munitions formulations and their fates in soils. Cold Regions Research and Engineering Laboratory, Hanover, NH, p 92

39 Dontsova KM, Yost SL, Simunek J, Pennington JC, Williford CW (2006) Dissolution and transport of TNT, RDX, and composition B in saturated soil columns. J Environ Qual 35:2043–2054

40 Thorn KA, Pennington JC, Kennedy KR, Cox LG, Hayes CA, Porter BE (2008) N-15 NMR study of the immobilization of 2,4- and 2,6-dinitrotoluene in aerobic compost. Environ Sci Technol 42:2542–2550

41 Pelletier P, Lavigne D, Laroche I, Cantin F, Phillips L, Fung V (2010) Additional properties studies of DNAN based melt-pour explosive formulations. In: 2010 insensitive munitions and energetic materials technology symposium, Munich, Germany

42 London JO, Smith DM (1985) A toxicological study of NTO. Los Alamos National Laboratory Report

43 Dontsova K, Taylor S (this volume) High explosives: their dissolution and fate in soils. In: Shukla M, Boddu V, Steevens J, Reddy D, Leszczynski J (eds) Energetic materials: from cradle to grave

44 Hawari J, Monteil-Rivera F, Perreault NN, Halasz A, Paquet L, Radovic-Hrapovic Z, Deschamps S, Thiboutot S, Ampleman G (2015) Environmental fate of 2,4-dinitroanisole (DNAN) and its reduced products. Chemosphere 119:16–23

45 Boparai H, Comfort S, Satapanajaru T, Szecsody J, Grossl P, Shea P (2010) Abiotic transformation of high explosives by freshly precipitated iron minerals in aqueous FeII solutions. Chemosphere 79:865–872

46 Dontsova KM, Hayes C, Pennington JC, Porter B (2009) Sorption of high explosives to water-dispersible clay: influence of organic carbon, aluminosilicate clay, and extractable iron. J Environ Qual 38:1458–1465

47 Spear RJ, Louey CN, Wolfson MG (1989) A preliminary assessment of 3-nitro-1,2,4-triazol-5-one (NTO) as an insensitive high explosive. DSTO Materials Research Laboratory, Maribyrnong, Australia, p 38

48 Brannon JM, Pennington JC (2002) Environmental fate and transport process descriptors for explosives. US Army Corps of Engineers, Engineer Research and Development Center, Vicksburg, MS

49 Linker BR, Khatiwada R, Perdrial N, Abrell L, Sierra R, Field JA, Chorover J (2015) Adsorption of novel insensitive munitions compounds at clay mineral and metal oxide surfaces. Environ Chem 12:74–84

50 Davies PJ, Provatas A (2006) Characterisation of 2,4-dinitroanisole: an ingredient for use in low sensitivity melt cast formulations. Weapons Systems Division, Defence Science and Technology Organisation

51 Coppola EN (2007) Treatment technologies for perchlorate. In: Global demil symposium

52 Sokkalingam N, Potoff JJ, Boddu VM, Maloney SW (2008) Prediction of environmental impact of high-energy materials with atomistic computer simulations. In: ADM002187. Proceedings of the army science conference (26th) held in Orlando, Florida on 1–4 Dec 2008

53 Dumitras-Hutanu CA, Pui A, Jurcoane S, Rusu E, Drochioiu G (2009) Biological effect and the toxicity mechanisms of some dinitrophenyl ethers. Rom Biotechnol Lett 14:4893–4899

54 Taylor S, Lever JH, Walsh ME, Fadden J, Perron N, Bigl S, Spanggord R, Curnow M, Packer B (2010) Dissolution rate, weathering mechanics and friability of TNT, Comp B, Tritonal, and Octol. ERDC/CRREL

55 Eriksson J, Skyllberg U (2001) Binding of 2,4,6-trinitrotoluene and its degradation products in a soil organic matter two-phase system. J Environ Qual 30:2053–2061

56 Stanley JK, Lotufo GR, Biedenbach JM, Chappell P, Gust KA (2015) Toxicity of the conventional energetics TNT and RDX relative to new insensitive munitions constituents DNAN and NTO in Rana pipiens tadpoles. Environ Toxicol Chem 34(4):873–879

57 Dodard SG, Sarrazin M, Hawari J, Paquet L, Ampleman G, Thiboutot S, Sunahara GI (2013) Ecotoxicological assessment of a high energetic and insensitive munitions compound: 2,4-dinitroanisole (DNAN). J Hazard Mater 262:143–150

58 Taylor S, Ringelberg DB, Dontsova K, Daghlian CP, Walsh ME, Walsh MR (2013) Insights into the dissolution and the three-dimensional structure of insensitive munitions formulations. Chemosphere 93:1782–1788

59 Yoon JM, Oliver DJ, Shanks JV (2005) Plant transformation pathways of energetic materials (RDX, TNT, DNTs). In: Eaglesham A, Bessin R, Trigiano R, Hardy RWT (eds) Agricultural biotechnology: beyond food and energy to health and the environment, national agricultural biotechnology council report 17. Ithaca, New York, National Agricultural Biotechnology Council, pp 103–116

60 Walsh MR, Walsh ME, Ramsey CA, Brochu S, Thiboutot S, Ampleman G (2013) Perchlorate contamination from the detonation of insensitive high-explosive rounds. J Hazard Mater 262:228–233

61 Motzer WE (2001) Perchlorate: problems, detection, and solutions. Environ Forensics 2:301–311

62 Le Campion L, Adeline MT, Ouazzani J (1997) Separation of NTO related 1,2,4-triazole-3-one derivatives by a high performance liquid chromatography and capillary electrophoresis. Propellants, Explos, Pyrotech 22:233–237

63 Walsh MR, Walsh ME, Poulin I, Taylor S, Douglas TA (2011) Energetic residues from the detonation of common US ordnance. Int J Energ Mater Chem Propul 10:169–186

64 Richard T, Weidhaas J (2014) Dissolution, sorption, and phytoremediation of IMX-101 explosive formulation constituents: 2,4-dinitroanisole (DNAN), 3-nitro-1,2,4-triazol-5-one (NTO), and nitroguanidine. J Hazard Mater 280:561–569

65 Lever JH, Taylor S, Perovich L, Bjella K, Packer B (2005) Dissolution of composition B detonation residuals. Environ Sci Technol 39:8803–8811

66 Taylor S, Lever JH, Fadden J, Perron N, Packer B (2009) Simulated rainfall-driven dissolution of TNT, Tritonal, comp B and Octol particles. Chemosphere 75:1074–1081

67 Park J, Comfort SD, Shea PJ, Machacek TA (2004) Remediating munitions-contaminated soil with zerovalent iron and cationic surfactants. J Environ Qual 33:1305–1313